Astročásticová fyzika – 3. přednáška:

Neutrina – problém deficitu slunečních neutrin, oscilace neutrin
Temná hmota – gravitační projevy – galaxie a jejich kupy,
silné a slabé čočkování, pokusy o přímou detekci,
roční modulace signálu v experimentu DAMA,
přebytek pozitronů pozorovaný družicí PAMELA
a přebytek elektronů z balonového experimentu ATIC

Celkové toky neutrin: Teorie vs. experimenty

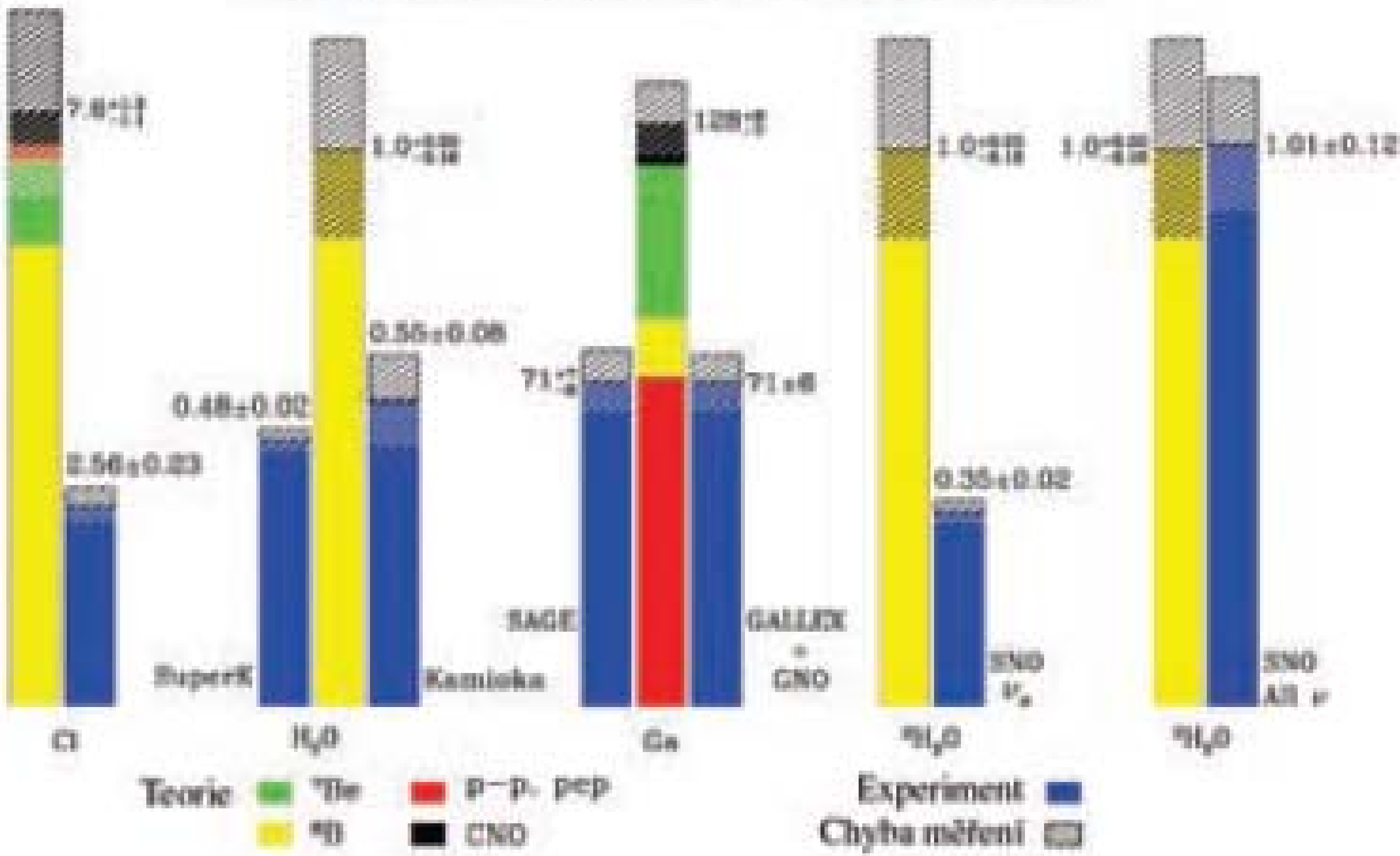

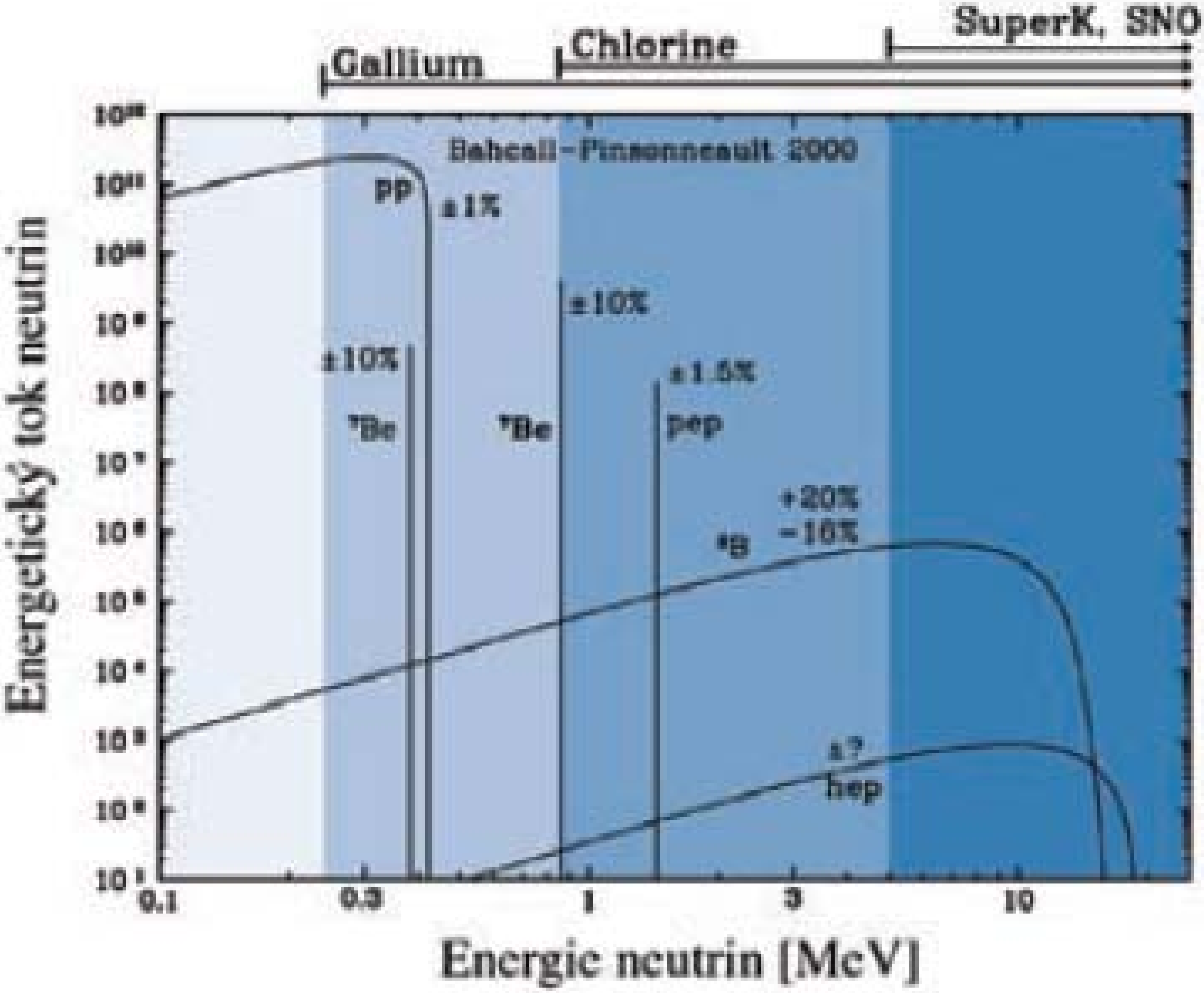
SuperK, SNO
Chlorine
Gallium
Bahcall-Pinsonneault 2000
pp
±1%
±10%
±10%
±1.5%
pep
+20%
−16%
±?
hep
0.1
0.3
1
3
10
Energetický tok neutrin
Energie neutrin [MeV]

Neutrino Mass

- Over the last decade, numerous experiments have indicated that neutrinos do have mass.
- These experiments exploit a quantum-mechanical phenomena – the probability of a neutrino of one type (there are three types of neutrinos) to change to a neutrino of a second type. This phenomena occurs ONLY if neutrinos of different types have different non-zero masses.

Neutrino Oscillation

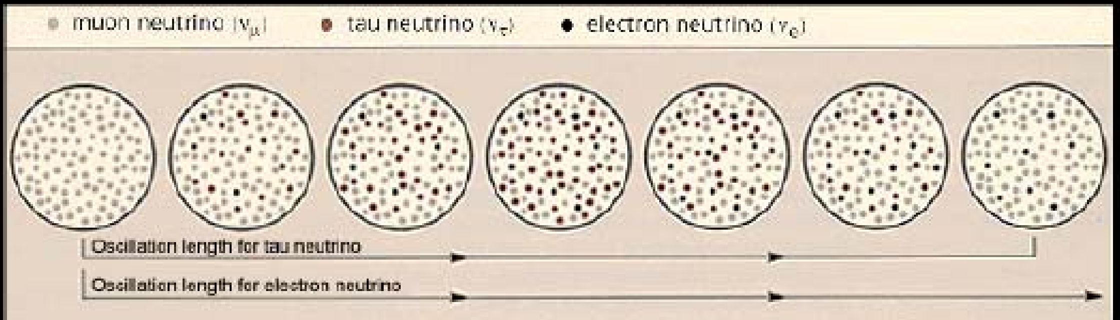

In this oscillation between muon (ν_μ), tau (ν_τ), and electron (ν_e) neutrinos, one "flavor" transforms into another and back again. There are different oscillation "potentials" for the electron and tau neutrinos (represented by their different-colored dots) and different lengths over which the oscillations occur.

- Neutrinos that are generated as one type 'morph' to neutrinos of one of the other two types as they travel.
- The probability that this transformation occurs depends upon the pathlength traveled, the energy of the neutrino, and the difference in mass between the two neutrino types.

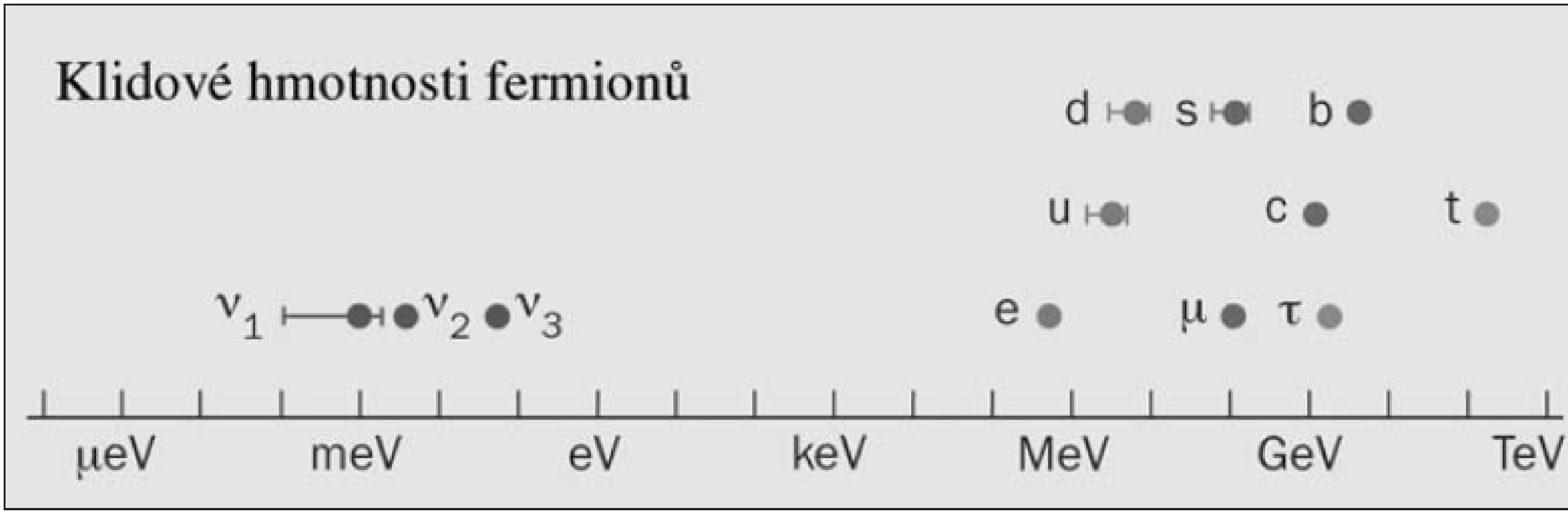
Klidové hmotnosti fermionů
d
s
b
u
c
t
ν1
ν2
ν3
e
μ
τ
μeV
meV
eV
keV
MeV
GeV
TeV

A example: MINOS

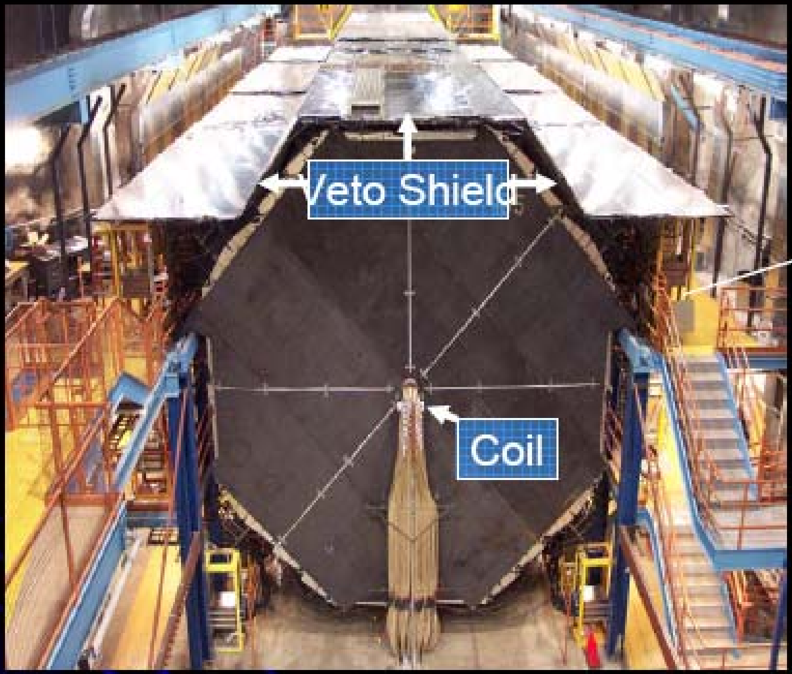

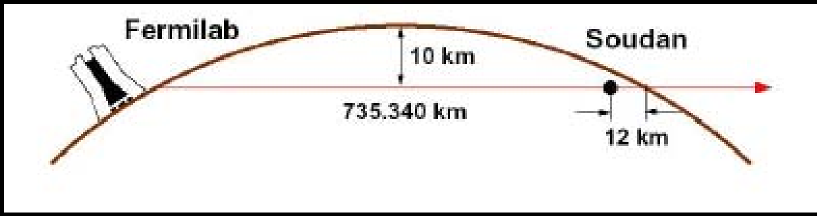

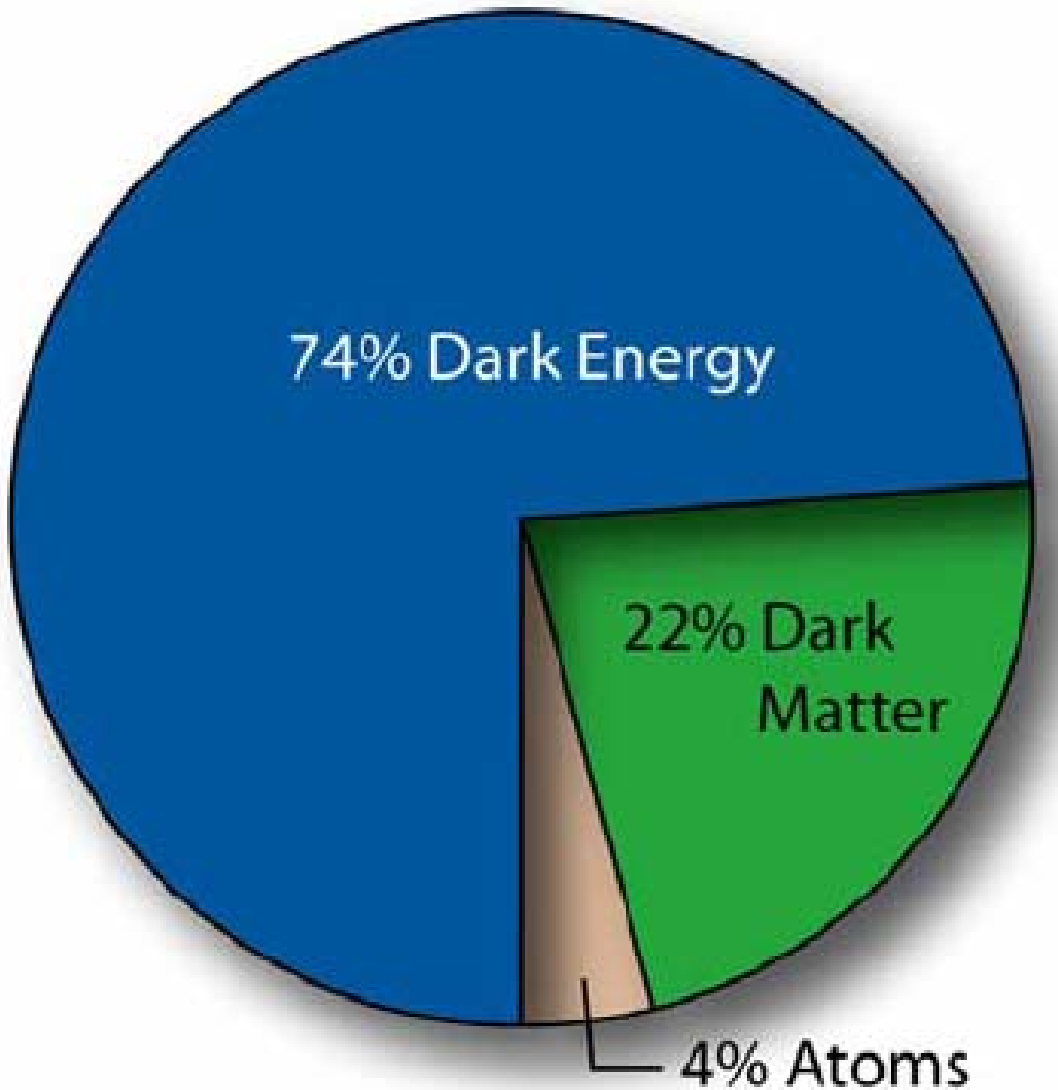
74% Dark Energy
22% Dark Matter
4% Atoms

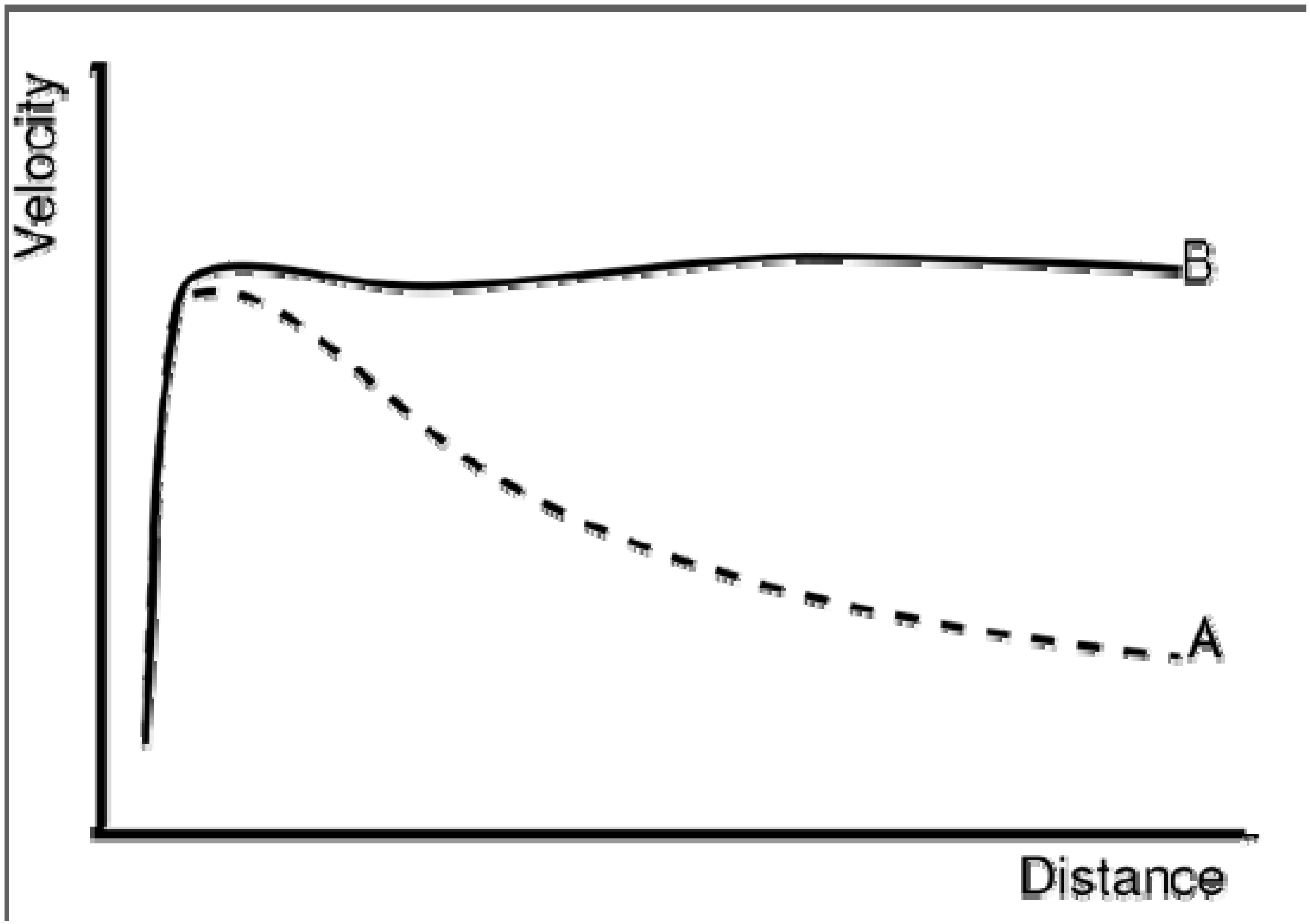
Velocity
B
A
Distance

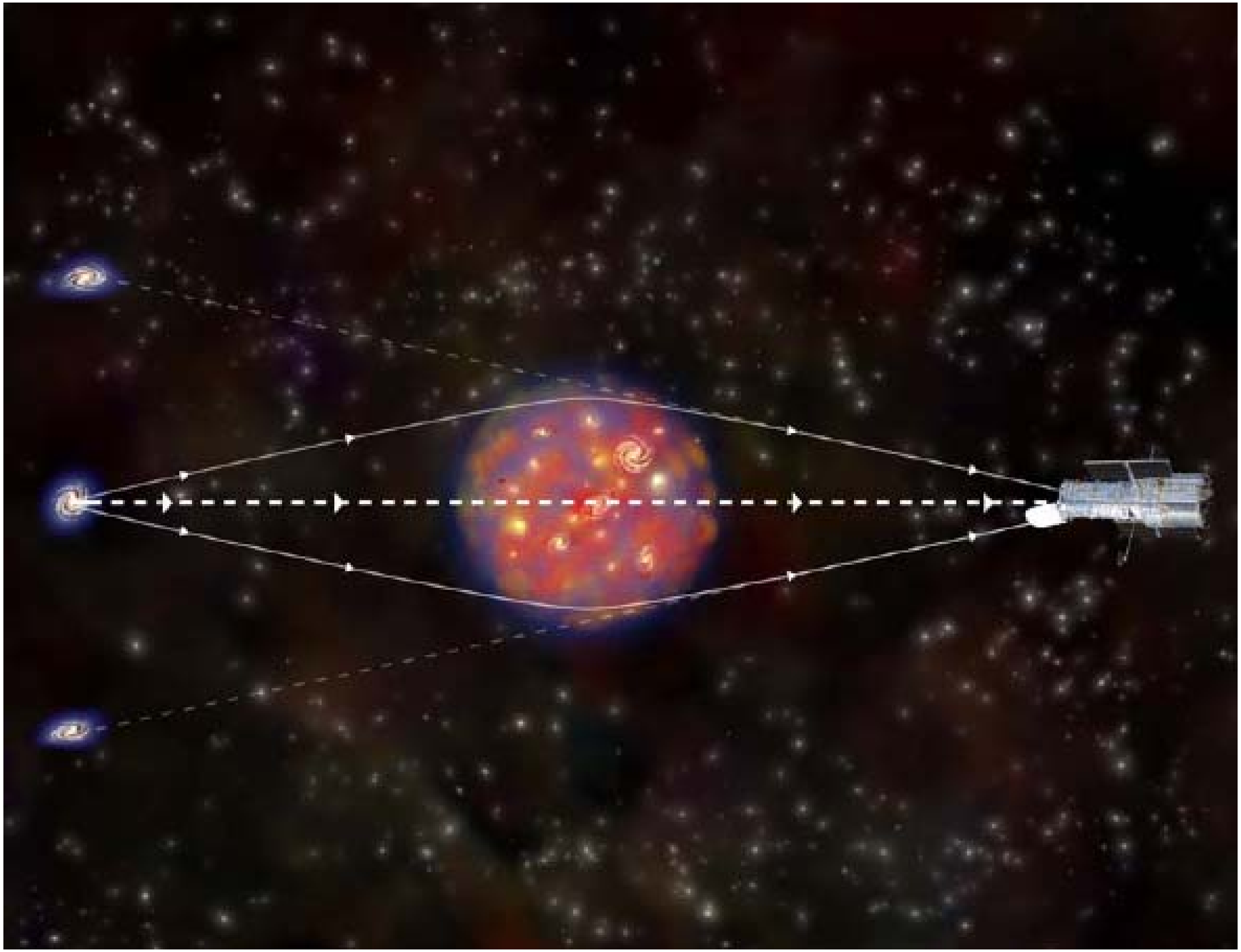

The Einstein Ring

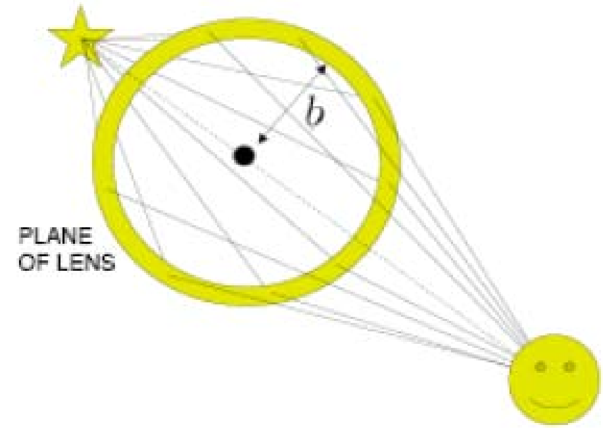

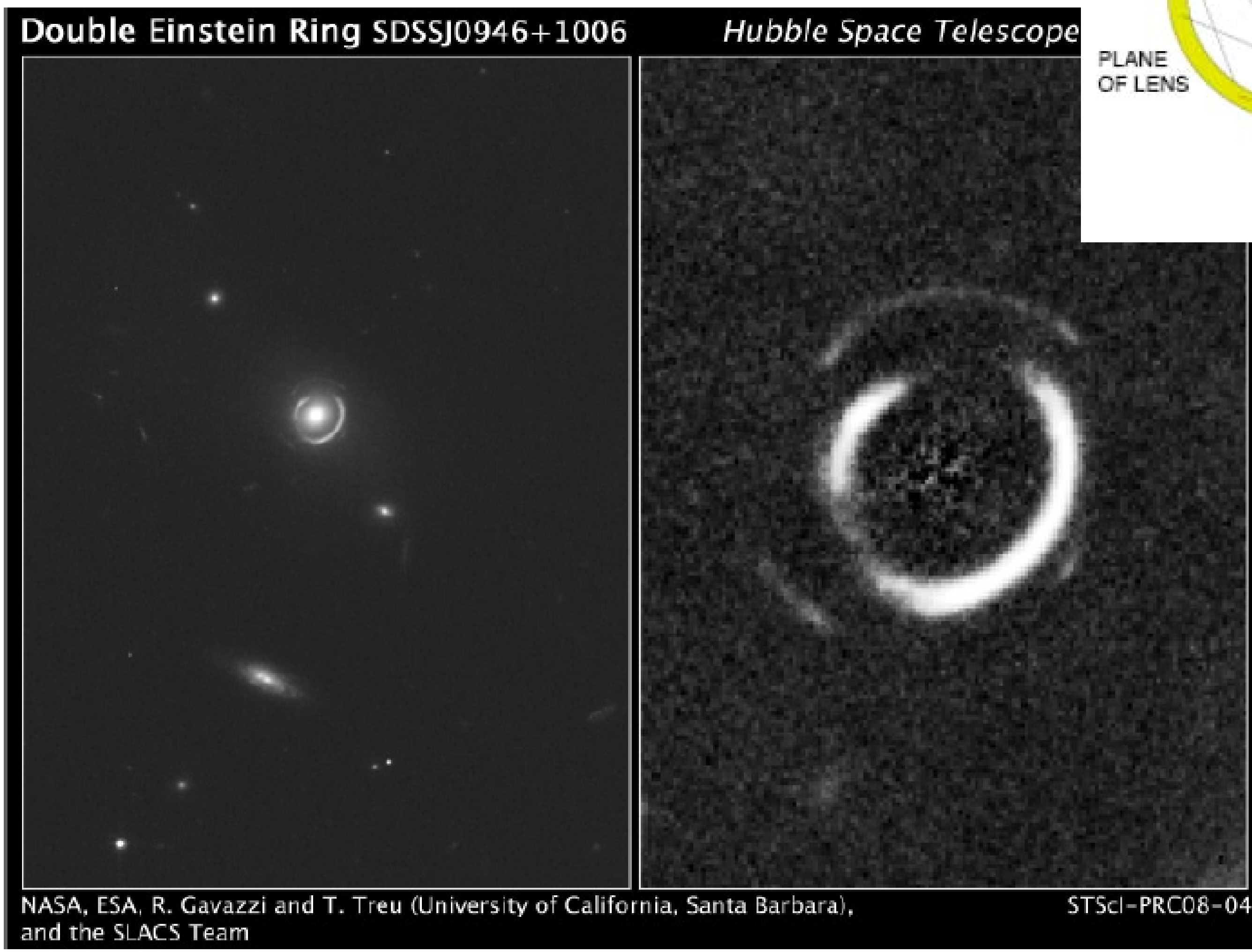

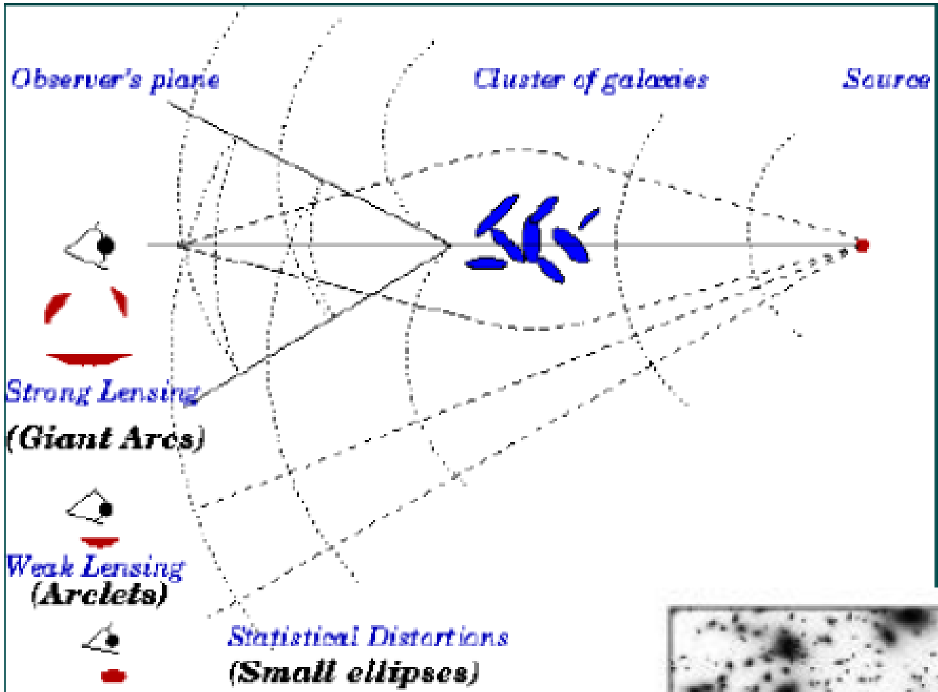

- deflection of light around massive objects

- sensitive to all mass not just luminous matter!

Weak Lensing Regime

Strong Lensing Regime

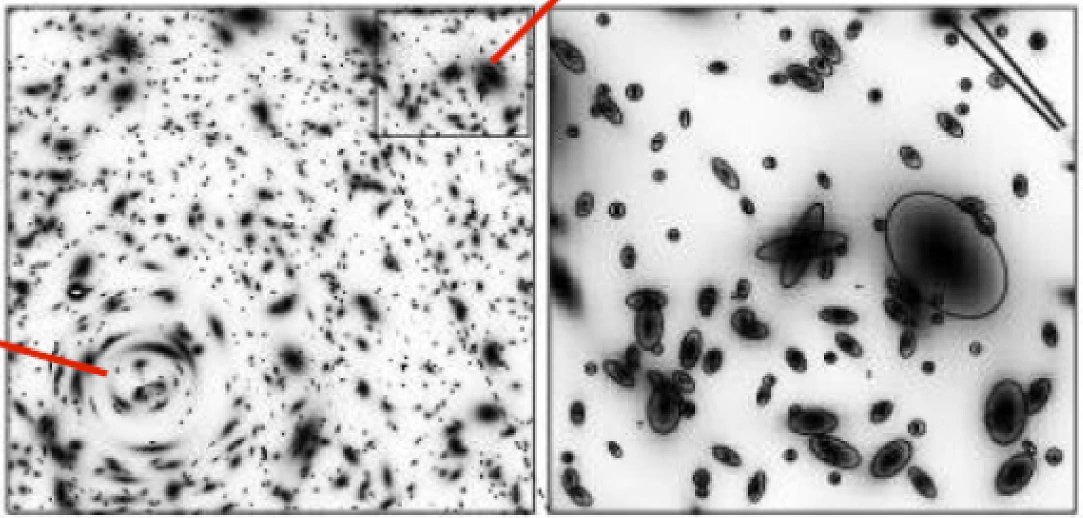

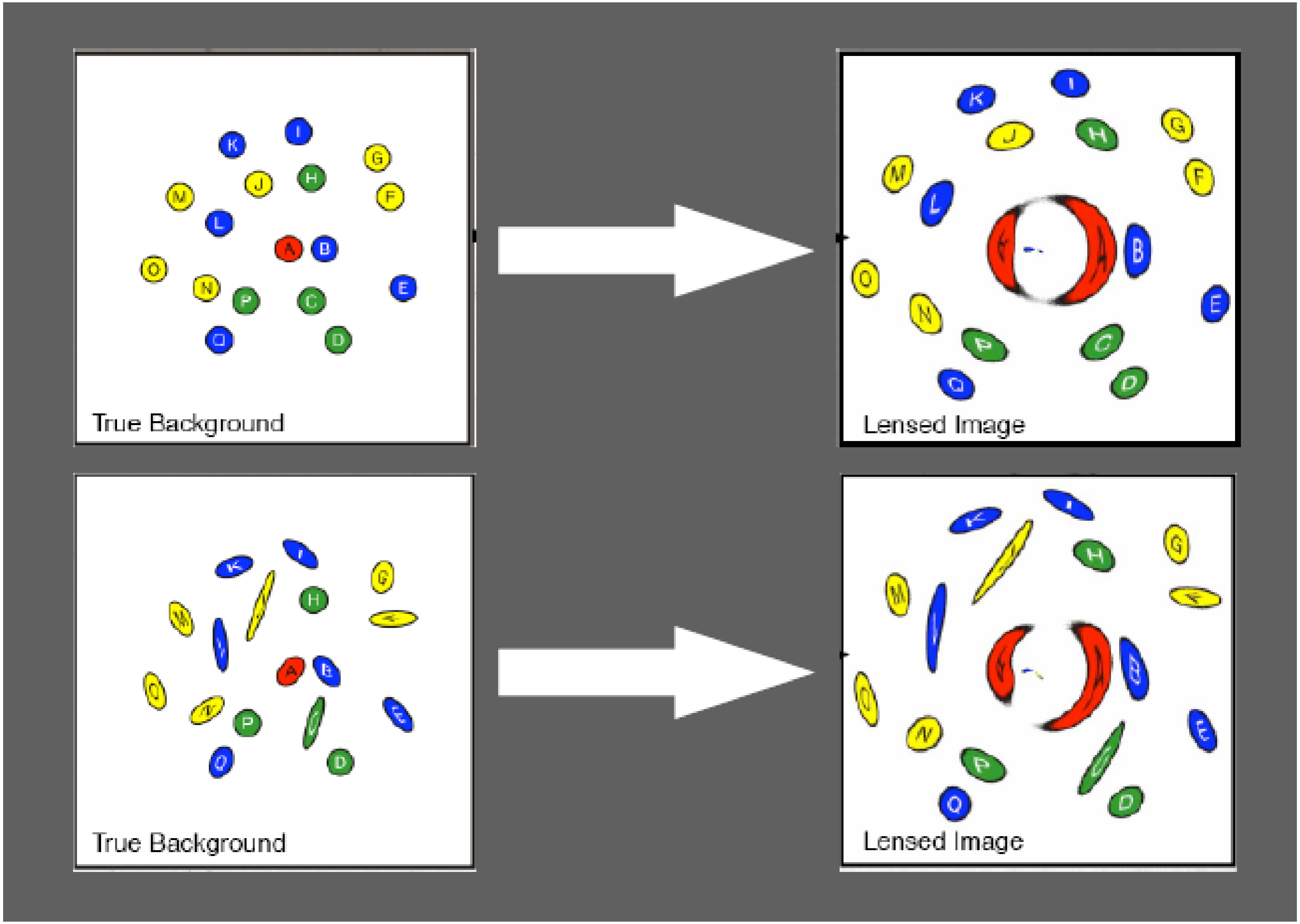
True Background
Lensed Image
True Background
Lensed Image

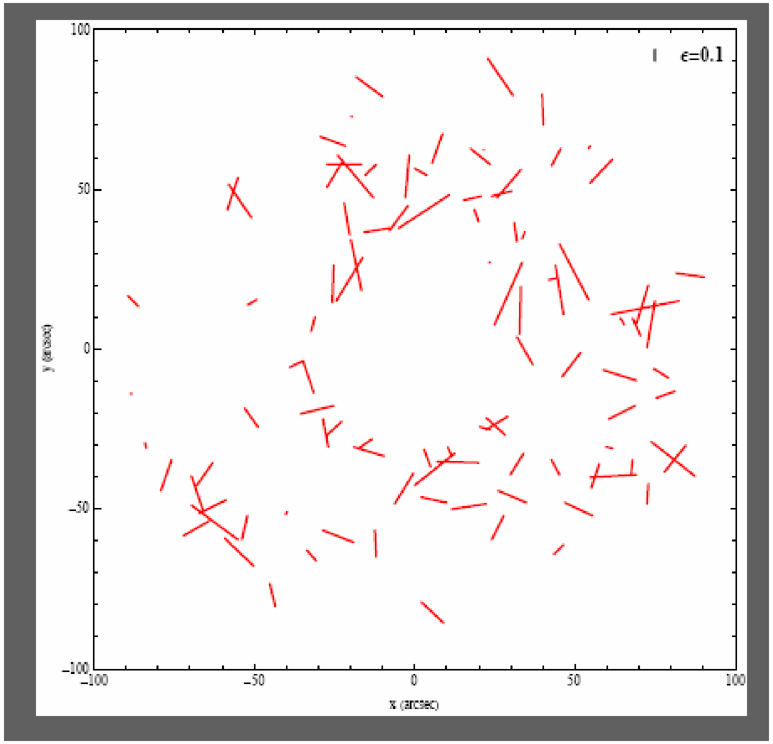

ϵ=0.1
y (arcsec)
x (arcsec)

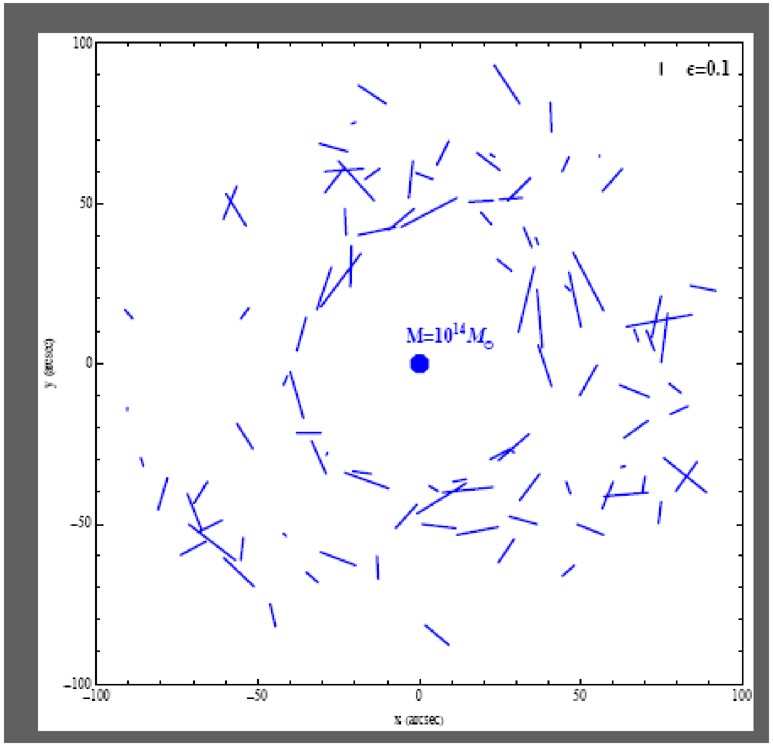

ϵ=0.1
M=10^14 M☉
y (arcsec)
x (arcsec)

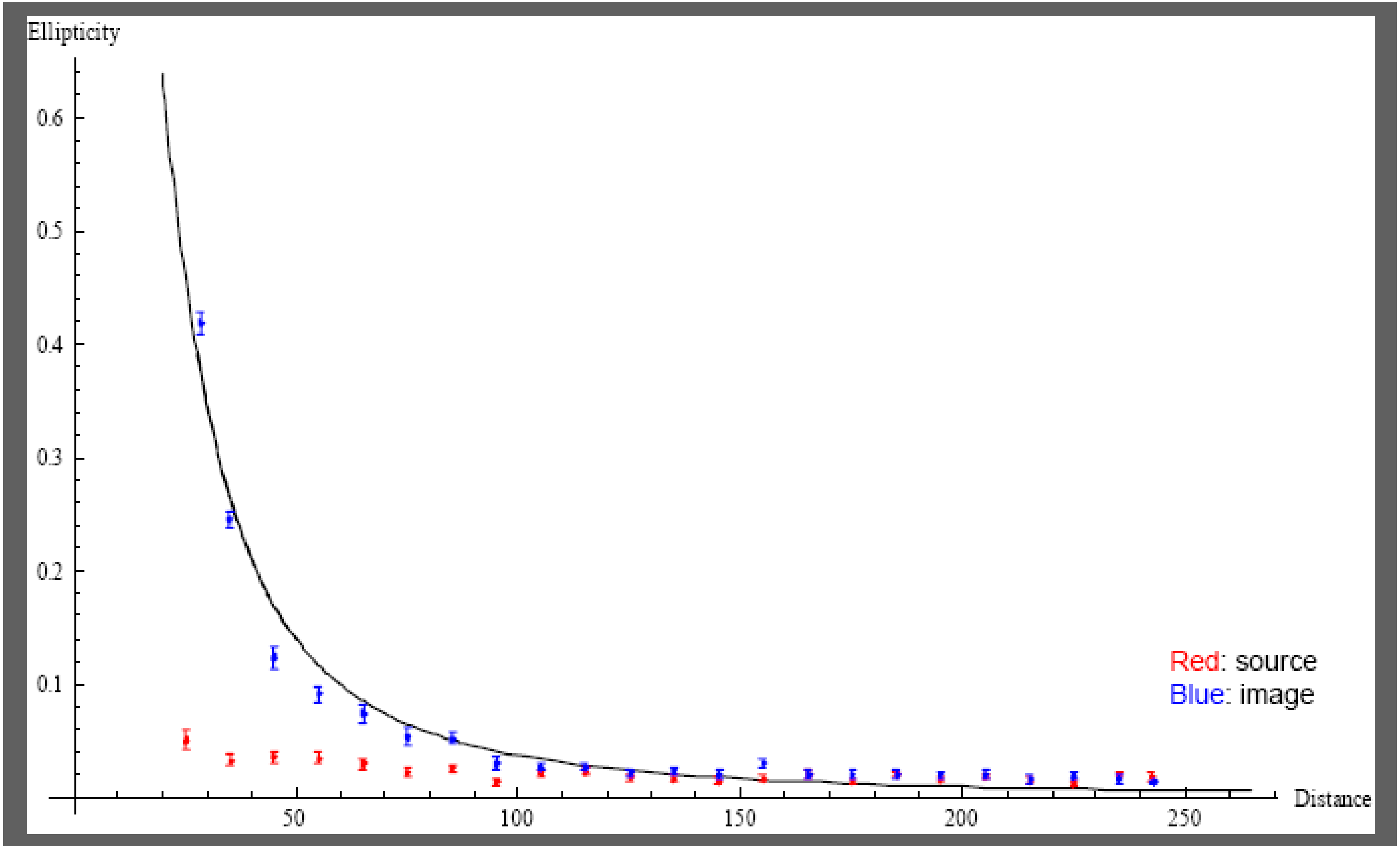
Ellipticity
0.6
0.5
0.4
0.3
0.2
0.1
50
100
150
200
250
Distance
Red: source
Blue: image

Shear field → reconstructed surface-mass density

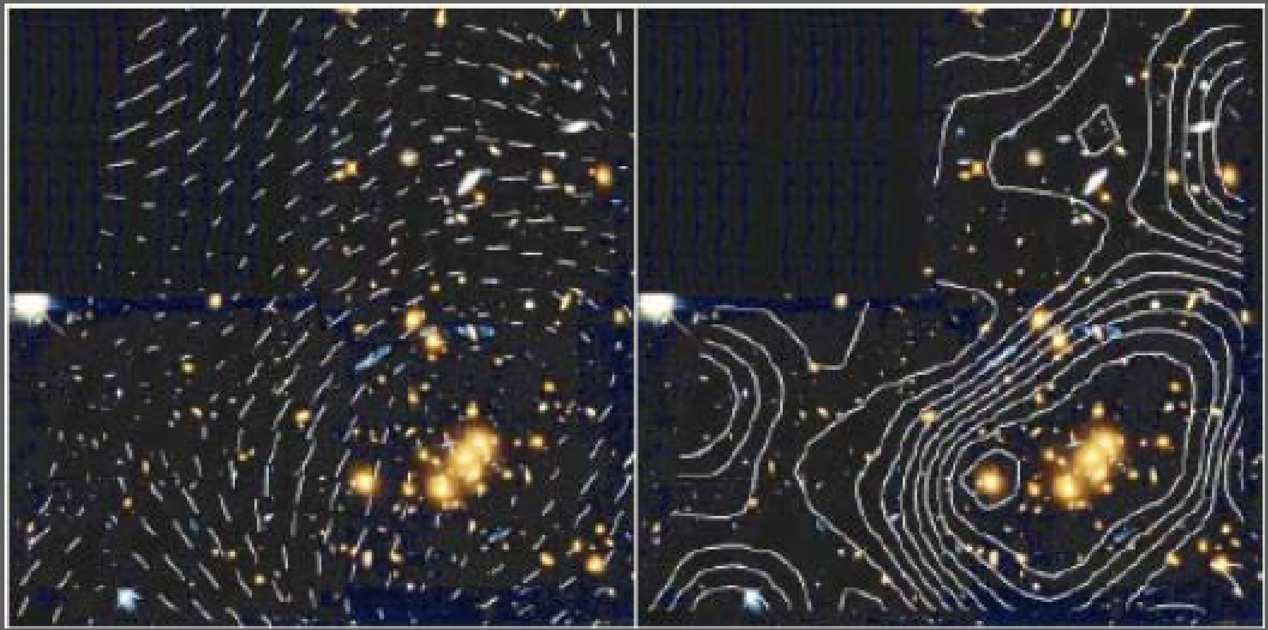

Credit: Y. Mellier & B. Fort; C. Seitz et al.

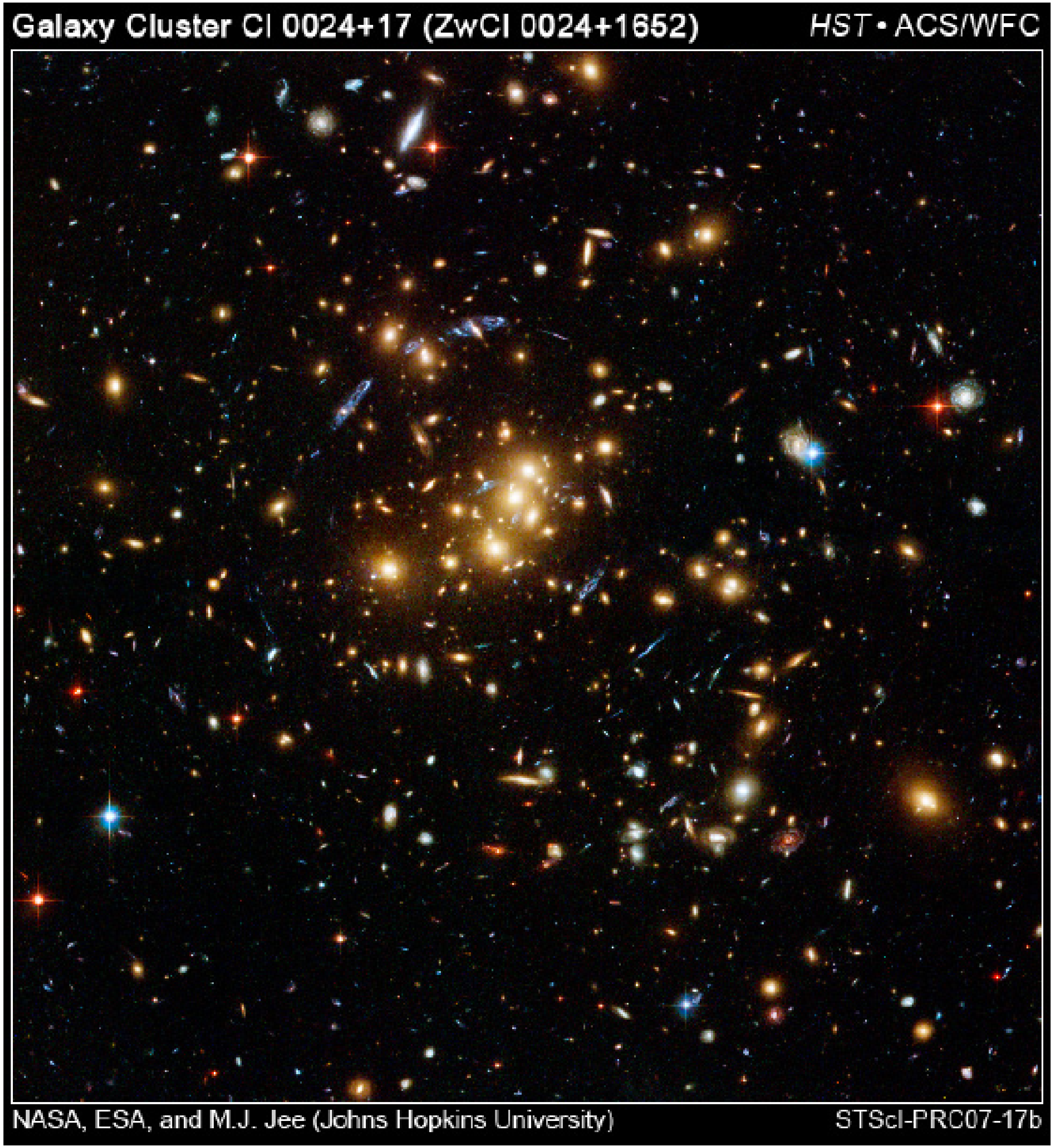
Galaxy Cluster Cl 0024+17 (ZwCl 0024+1652)
HST • ACS/WFC
NASA, ESA, and M.J. Jee (Johns Hopkins University)
STScI-PRC07-17b

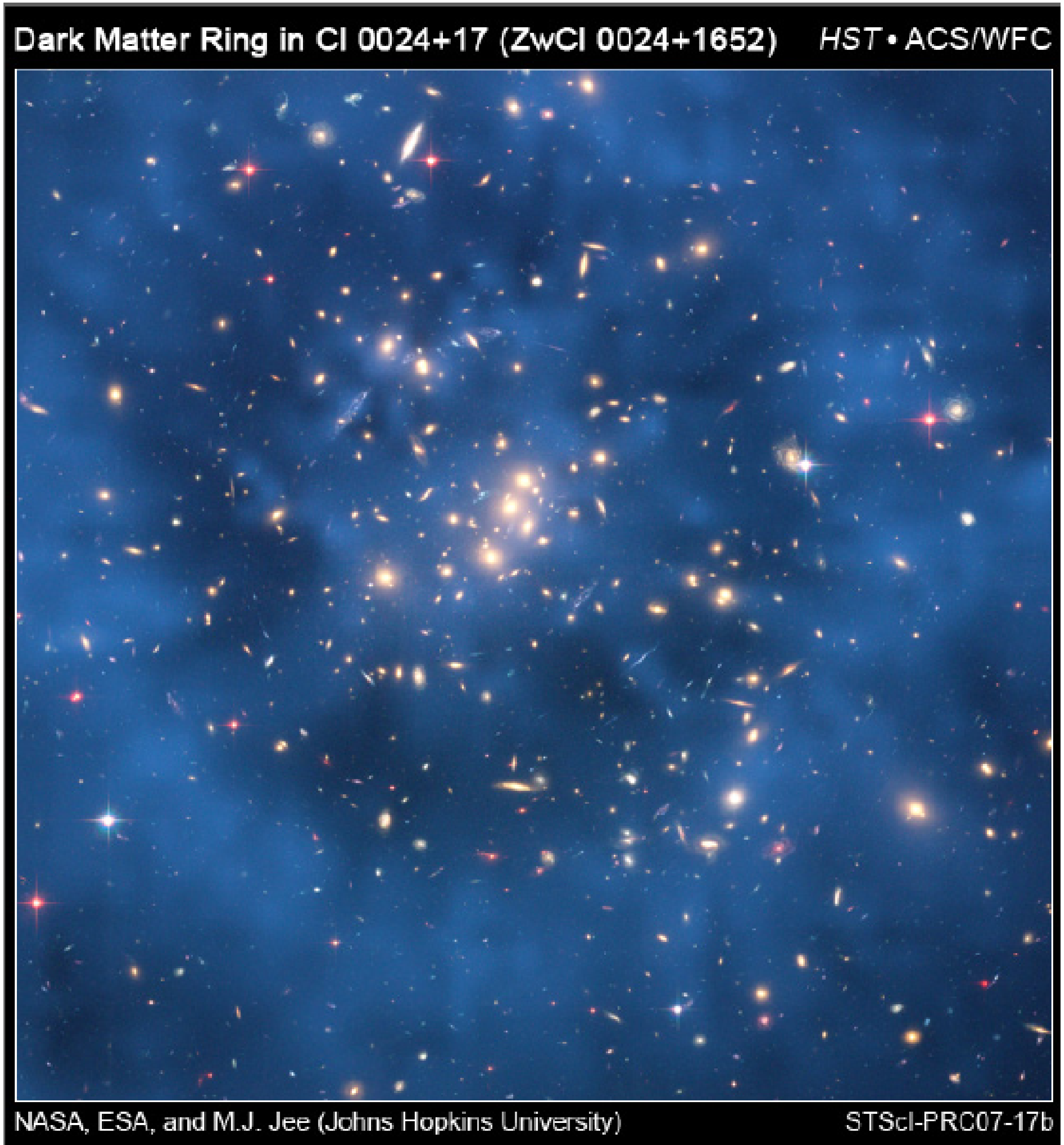
Dark Matter Ring in Cl 0024+17 (ZwCl 0024+1652)
HST • ACS/WFC
NASA, ESA, and M.J. Jee (Johns Hopkins University)
STScI-PRC07-17b


Dark matter search strategies
WIMP
1. Direct detection >
Milky way
2. Indirect detection >
WIMP
WIMP
γ
ν
Sun
Earth
< 3. Production at the Large Hadron Collider

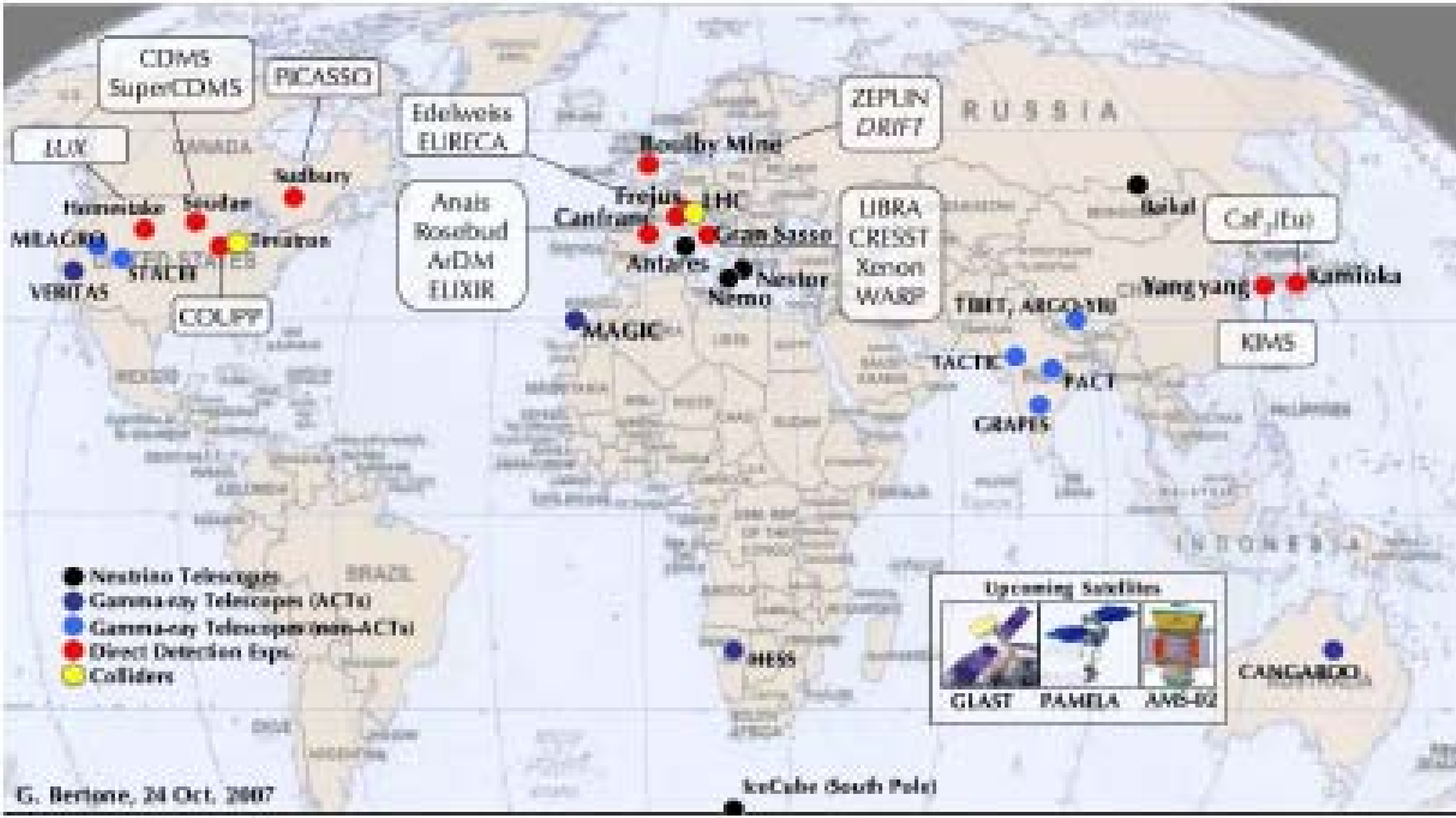

CDMS
SuperCDMS
PICASSO
LUX
Edelweiss
EURECA
ZEPLIN
DRIFT
RUSSIA
Boulby Mine
Sudbury
Homestake
Soudan
Frejus
LHC
Canfranc
Gran Sasso
Antares
Nestor
Nemo
Baikal
Anais
Rosebud
ArDM
ELIXIR
LIBRA
CRESST
Xenon
WARP
MILAGRO
STACEE
Tevatron
VERITAS
COUPP
MAGIC
TIBET, ARGO-YBJ
TACTIC
PACT
GRAPES
Yangyang
Kamioka
KIMS
BRAZIL
Neutrino Telescopes
Gamma-ray Telescopes (ACTs)
Gamma-ray Telescopes (non-ACTs)
Direct Detection Exps.
Colliders
HESS
Upcoming Satellites
GLAST
PAMELA
AMS-02
CANGAROO
G. Bertone, 24 Oct. 2007
IceCube (South Pole)

Sources of Background

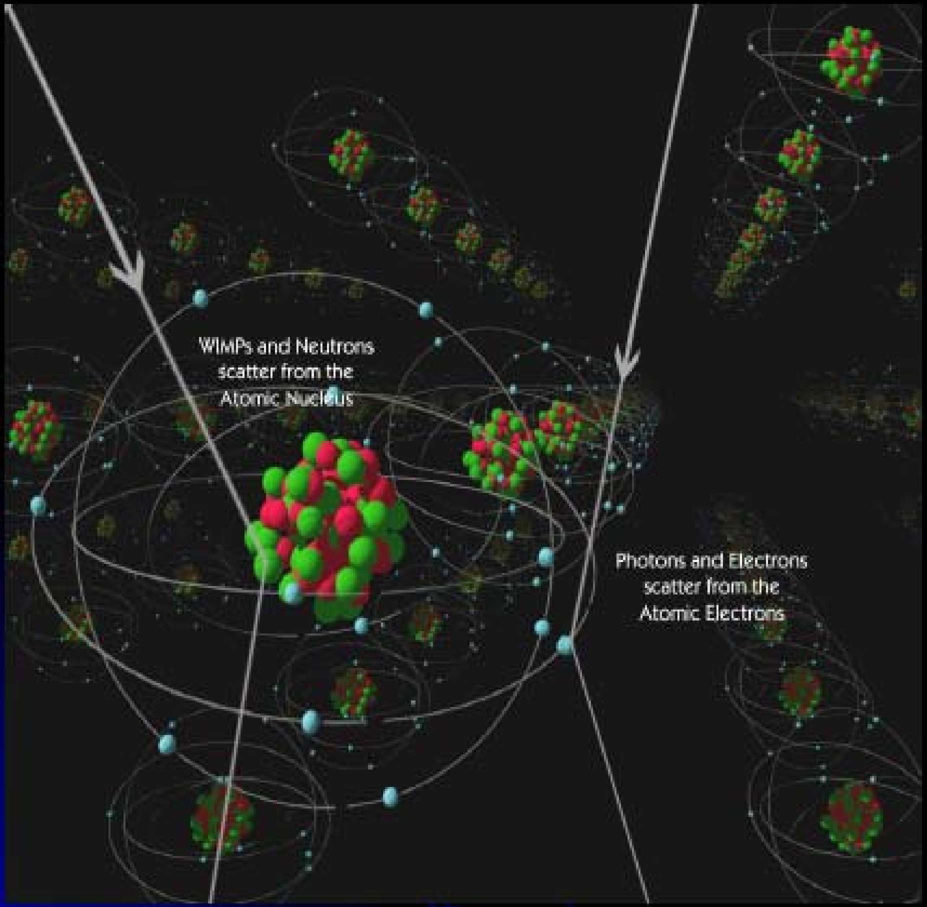

Detectors must effectively discriminate between

Nuclear Recoils (Neutrons, WIMPs)

Electron Recoils (gammas, betas)

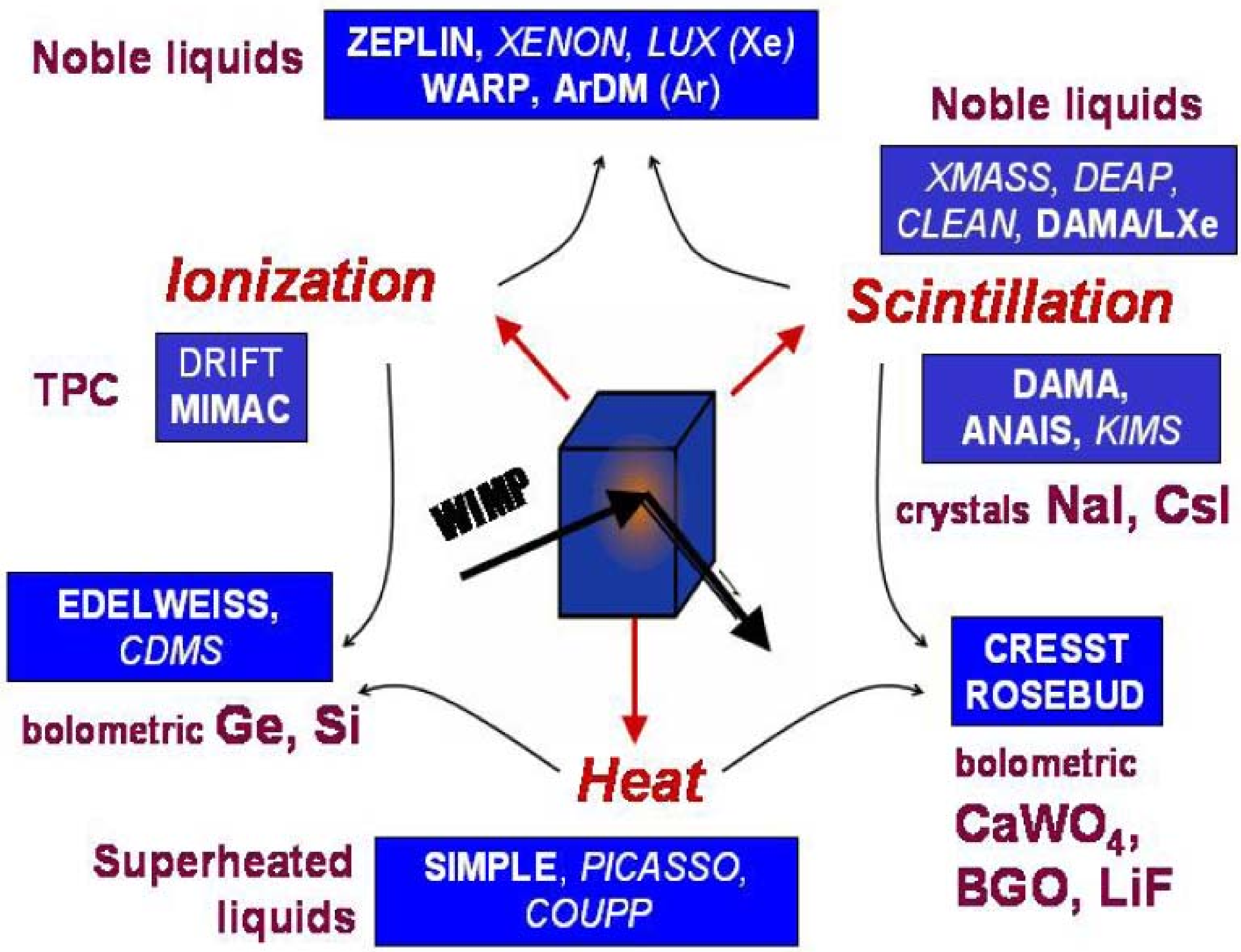
Noble liquids
ZEPLIN, XENON, LUX (Xe)
WARP, ArDM (Ar)
Noble liquids
XMASS, DEAP,
CLEAN, DAMA/LXe
Ionization
Scintillation
TPC
DRIFT
MIMAC
DAMA,
ANAIS, KIMS
WIMP
crystals NaI, CsI
EDELWEISS,
CDMS
CRESST
ROSEBUD
bolometric Ge, Si
Heat
bolometric
CaWO4,
BGO, LiF
Superheated
liquids
SIMPLE, PICASSO,
COUPP

Direct Cold Dark Matter Detection

- CDM particles are very heavy (100's of times heavier than a proton) they have a low velocity wrt the speed of light. That means, when we 'swim' through the sea of CDM particles as the sun orbits the center of the galaxy, and the Earth orbits the sun, the velocity of the CDM relative to us changes with the time of year. In June, the Sun's motion in the Galaxy is aligned with the Earth's motion about the sun, and the apparent velocity of CDM particles increases. In December, the two velocities are opposed. This effects the event rates seen in Dark Matter detectors, and we expect this event rate to modulate with the time of year.

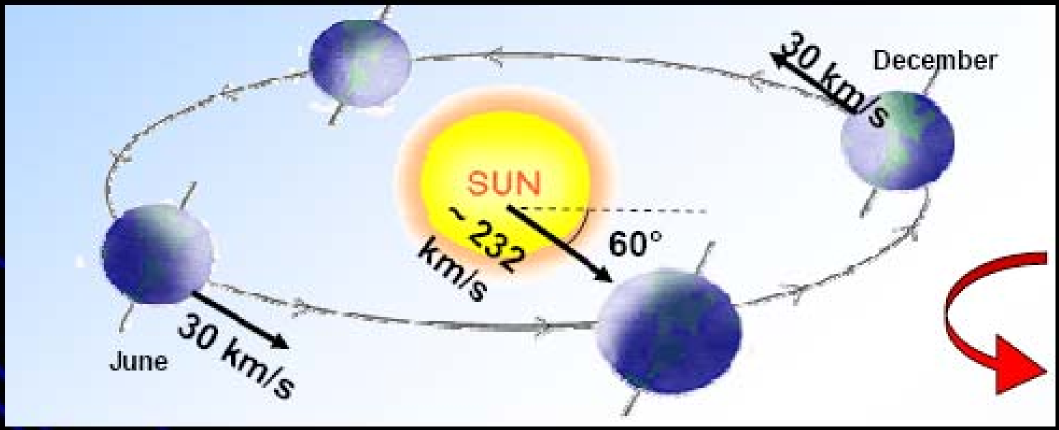

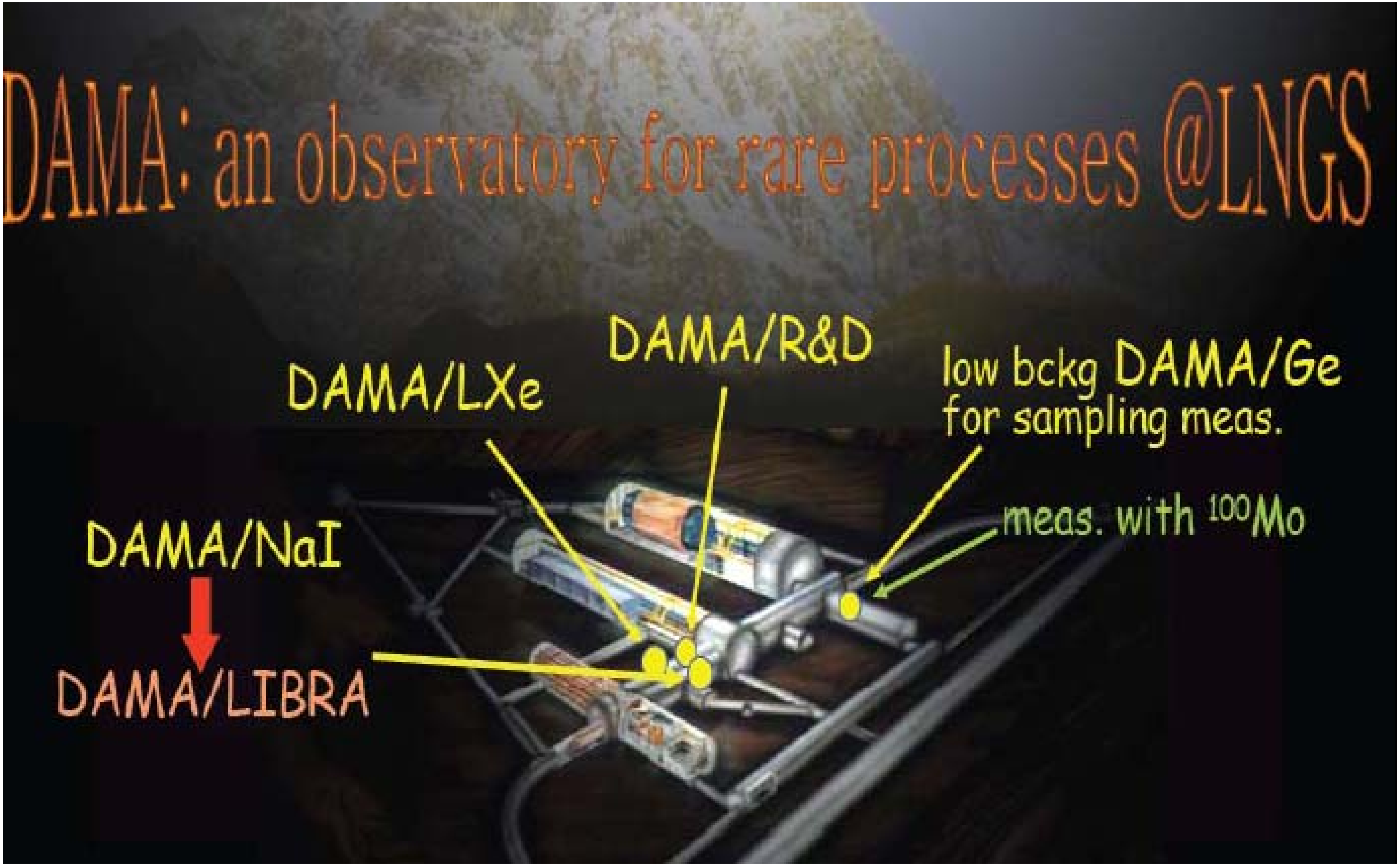

DAMA: an observatory for rare processes @LNGS
DAMA/R&D
DAMA/LXe
low bckg DAMA/Ge
for sampling meas.
meas. with 100Mo
DAMA/NaI
DAMA/LIBRA

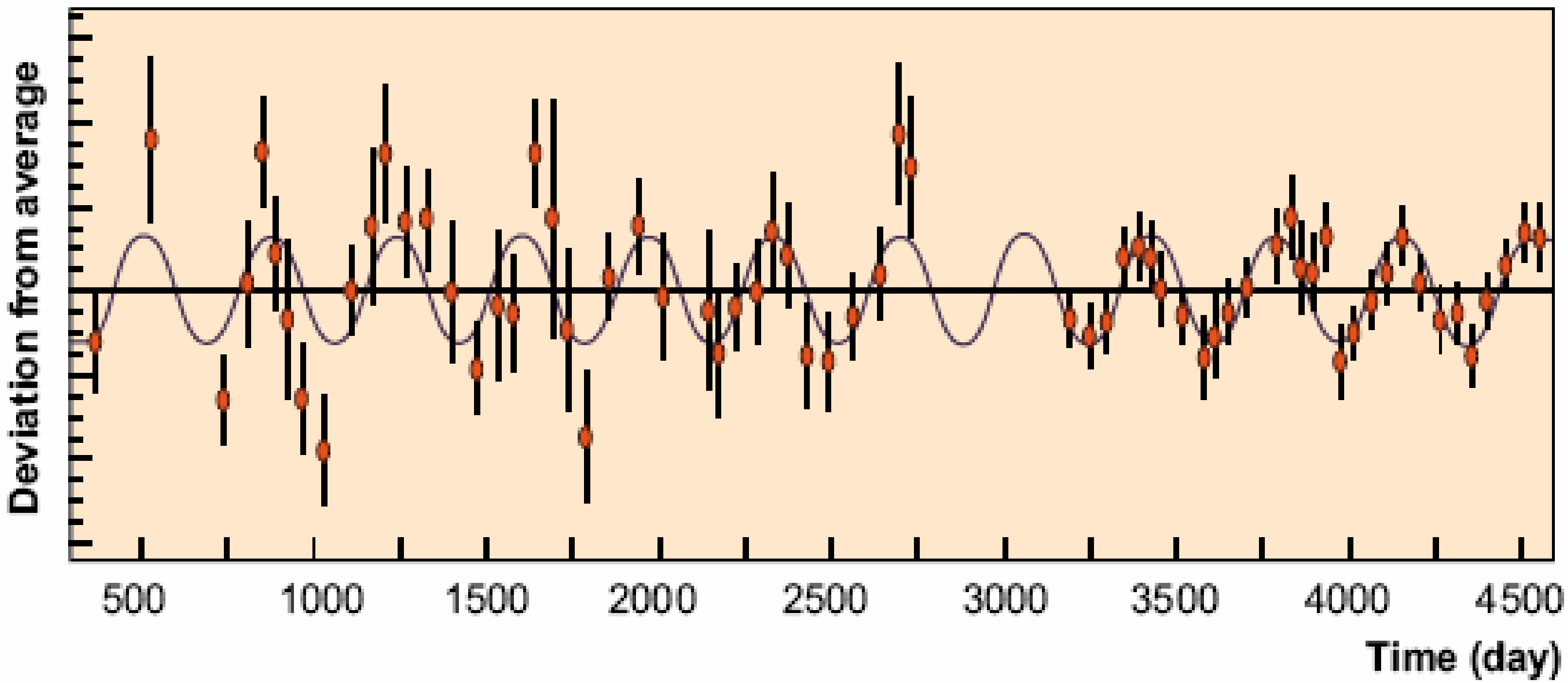
Deviation from average
500
1000
1500
2000
2500
3000
3500
4000
4500
Time (day)

CDMS – the current state of the art

- CDMS (Cold Dark Matter Search), is a solid state detector now taking data in the Soudan Mine in northern Minnesota.
- The CDMS detector is unique in it's ability to distinguish signals from Dark Matter particles from gamma signals originating for radioactive decay of nearby material.

CDMS II Limit

Event rates in DM detection depends up mass of DM particle, and strength of interaction between DM particle and normal matter. Neither are known, and so when no signal is seen the experiment places limits on allowed possibilities for mass and interaction strength. The CDMS experiment has ruled out the range of values allowed by the earlier DAMA result.

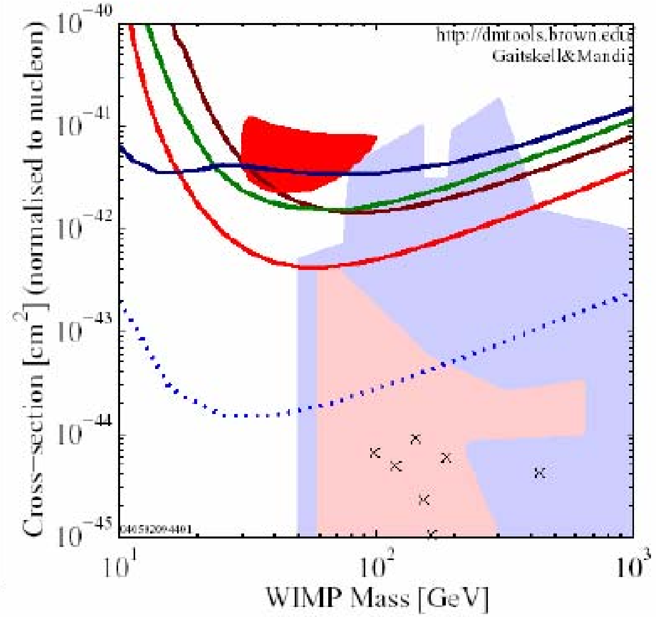

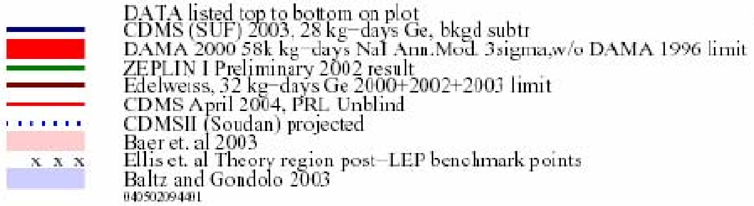

The Future of Direct Dark Matter Searches – Cryogenic Detectors

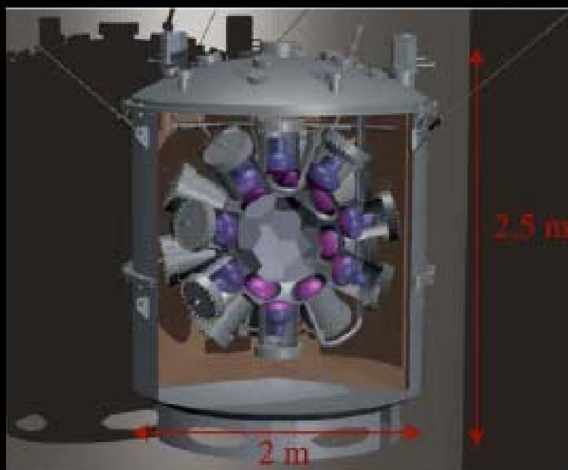

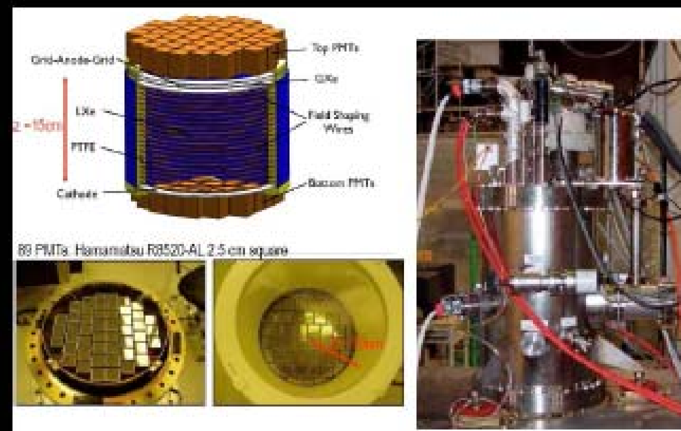

- Solid state detectors like CDMS hard to scale up in size. Future detectors are likely to use cryogenic liquids (Xe or Ar) as the active volume.
- Next generation detectors will be 100 kg active mass, a factor of 10 larger than CDMS. The ultimate goal for DUSEL is 2-10 tonne – class detectors, that will be factor of ~1000 more sensitive than CDMS.
- This field is now moving very rapidly, and chances are extremely good that dark matter will be detected in the lab within the next 10-15 years.

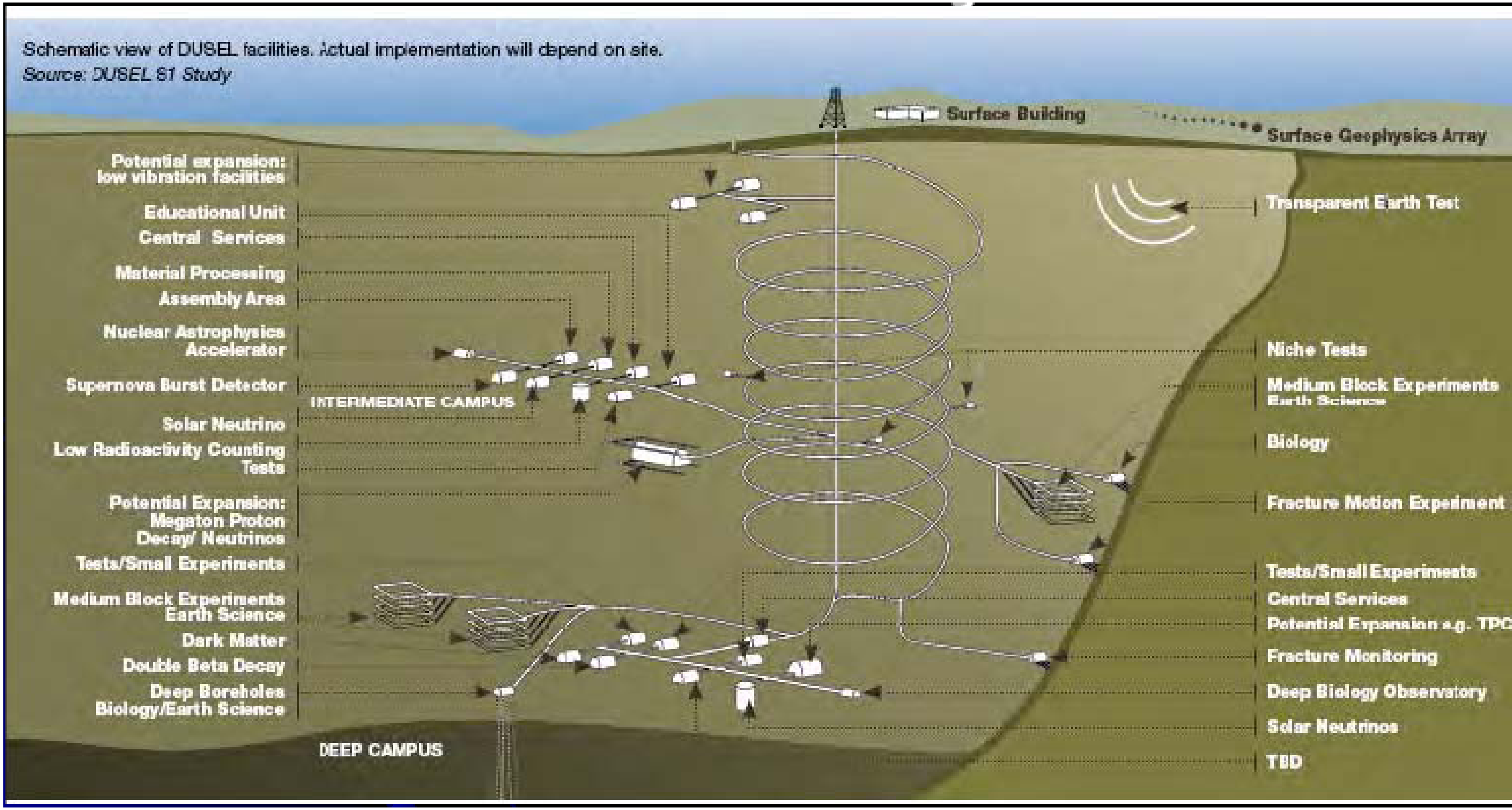

Schematic view of DUSEL facilities. Actual implementation will depend on site.
Source: DUSEL S1 Study

Annihilations of neutralinos (majorana fermions; i.e. their antiparticles are identical)

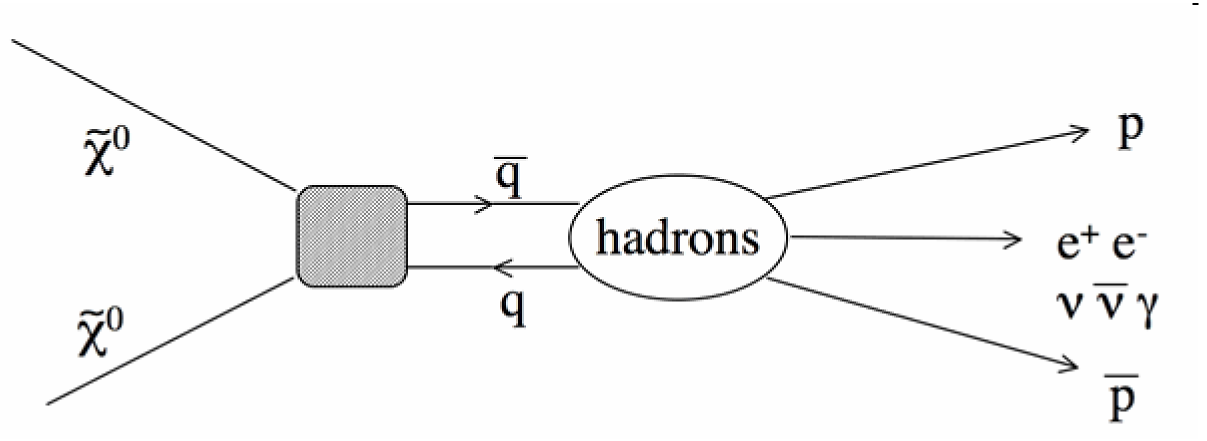

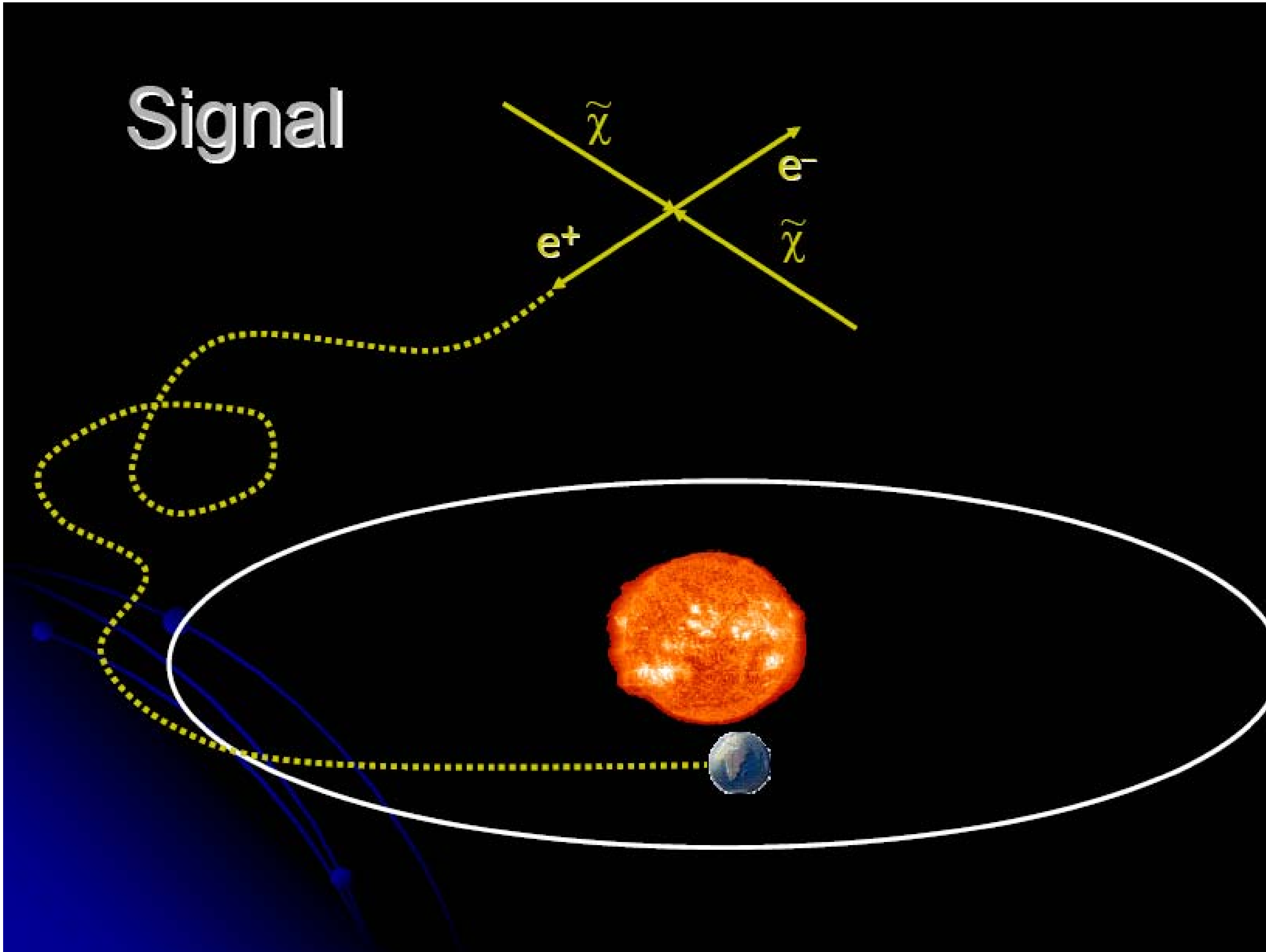
Signal
$\tilde{\chi}$
e^-
e^+
$\tilde{\chi}$

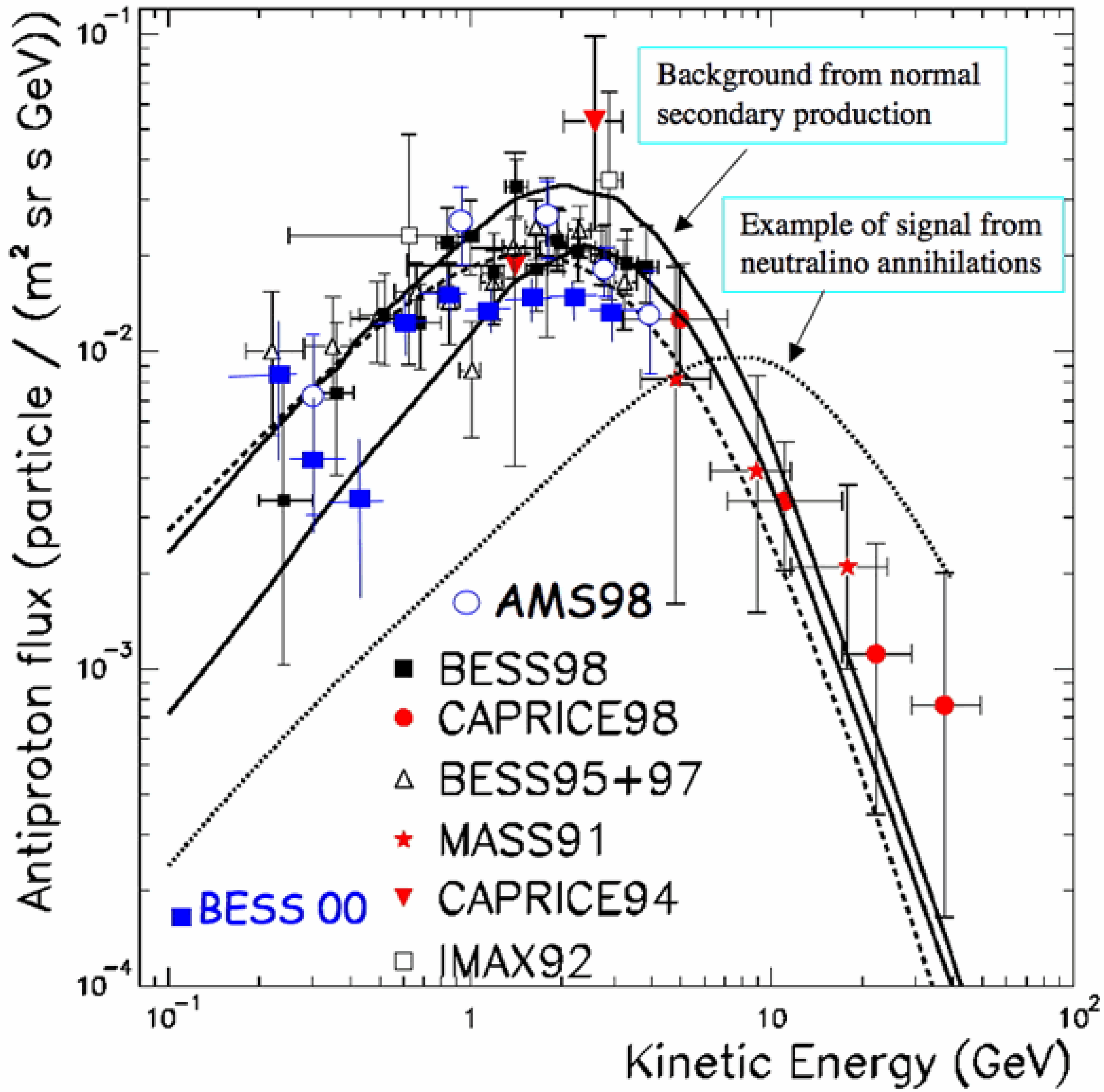
Background from normal secondary production
Example of signal from neutralino annihilations
Antiproton flux (particle / (m² sr s GeV))
Kinetic Energy (GeV)
10⁻¹
10⁻²
10⁻³
10⁻⁴
10⁻¹
1
10
10²
AMS98
BESS98
CAPRICE98
BESS95+97
MASS91
CAPRICE94
IMAX92
BESS 00

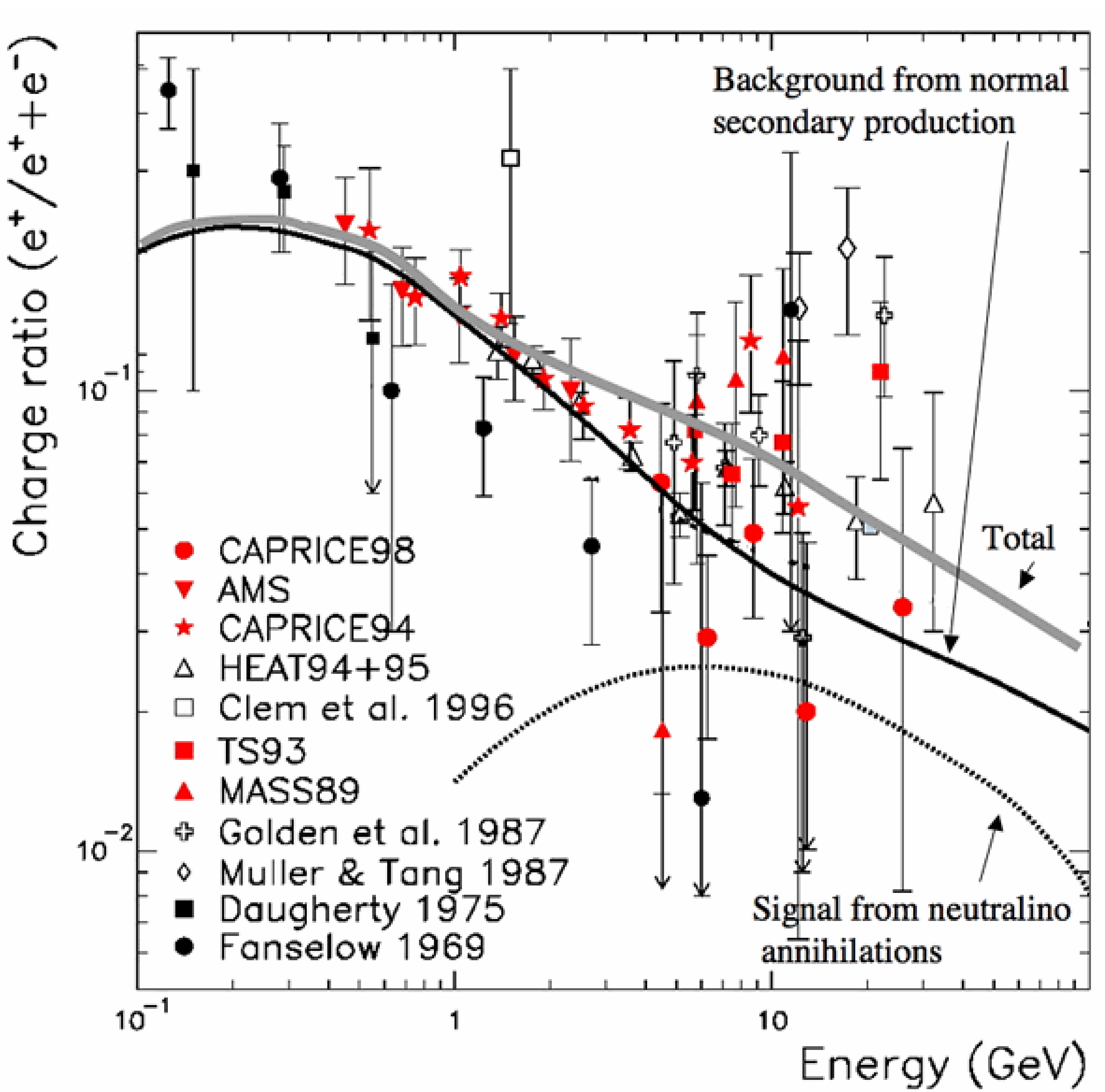

Charge ratio (e+/e++e-)
Energy (GeV)
Background from normal secondary production
Total
Signal from neutralino annihilations
CAPRICE98
AMS
CAPRICE94
HEAT94+95
Clem et al. 1996
TS93
MASS89
Golden et al. 1987
Muller & Tang 1987
Daugherty 1975
Fanselow 1969

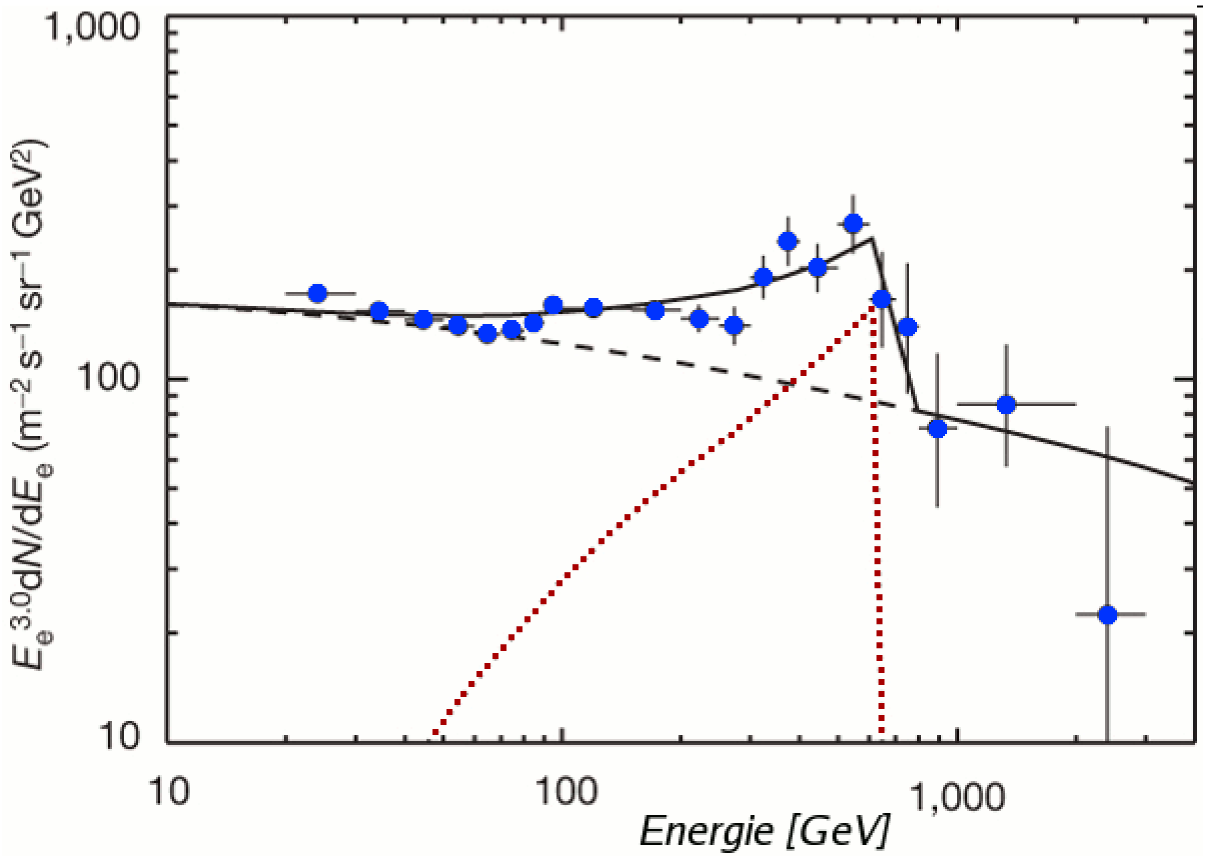

1,000
100
10
10
100
1,000
Energie [GeV]
$E_e^{3.0} dN/dE_e$ (m^{-2} s^{-1} sr^{-1} GeV^2)

Družice PAMELA

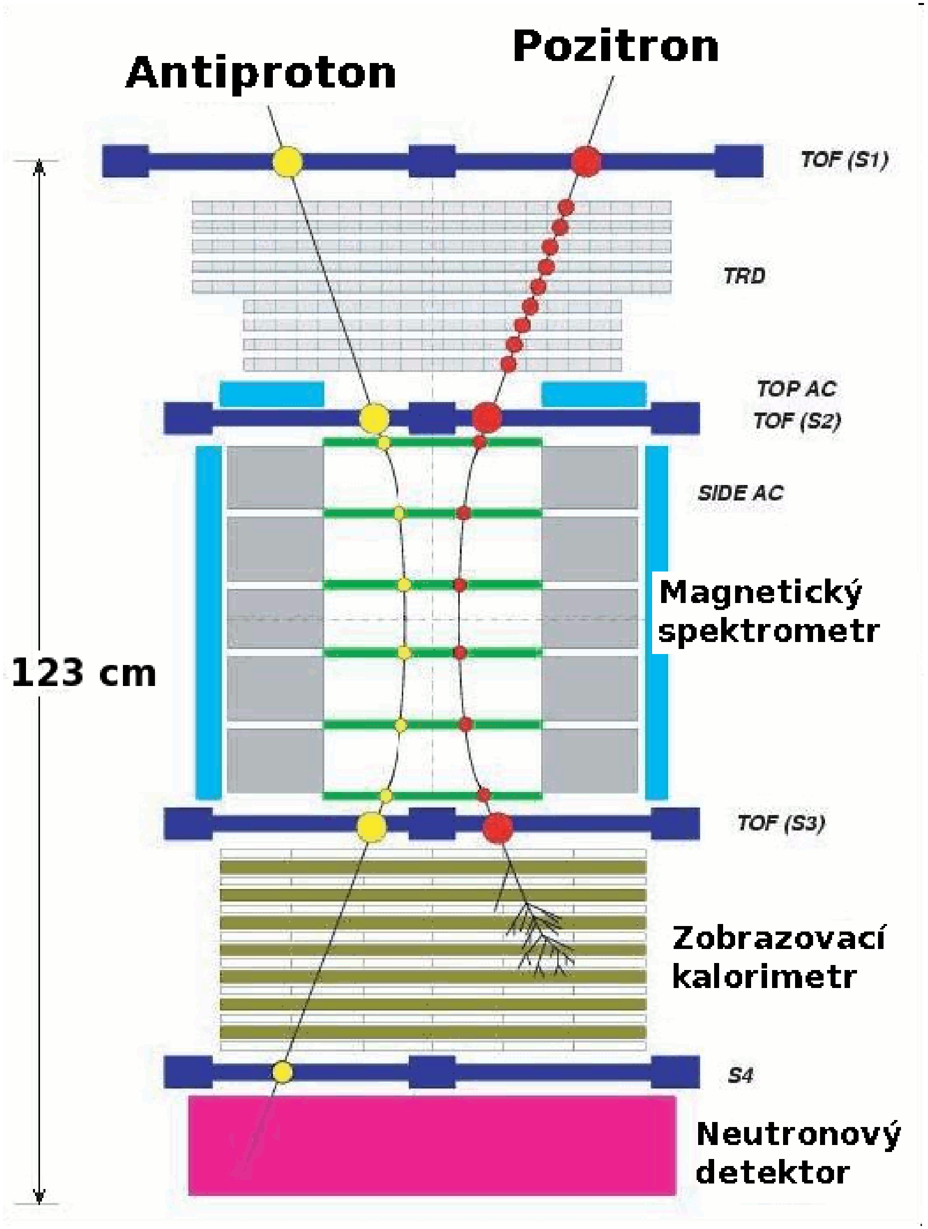

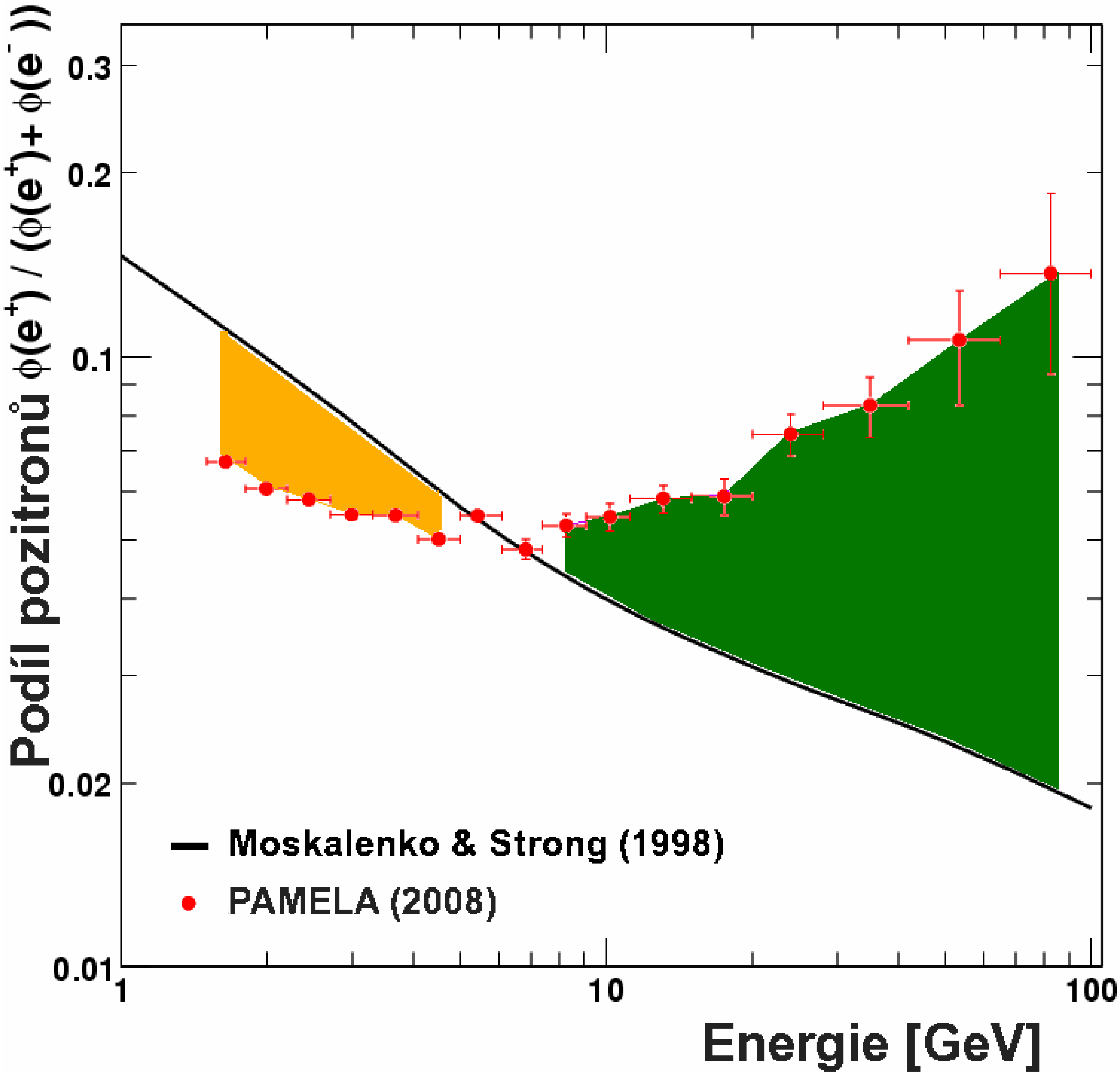

Podíl pozitronů ϕ(e+) / (ϕ(e+)+ϕ(e-))
0.3
0.2
0.1
0.02
0.01
1
10
100
Energie [GeV]
Moskalenko & Strong (1998)
PAMELA (2008)

Astročásticová fyzika – 4. přednáška:

Neutrina – ještě douška k oscilacím
Gravitační vlny – nepřímé projevy a pozorování pulzarů, typické amplitudy, detektory gravitačních vln – LIGO, LISA
Gravitace a její měření na malých škálách – hledání možných projevů extradimenzí
Proměnlivé konstanta – proměnlivá konstanta jemné struktury, pozorování spektrálních čar kvasarů

$$
\begin{aligned}
U &= \begin{bmatrix} U_{e1} & U_{e2} & U_{e3} \\ U_{\mu1} & U_{\mu2} & U_{\mu3} \\ U_{\tau1} & U_{\tau2} & U_{\tau3} \end{bmatrix} \\
&= \begin{bmatrix} 1 & 0 & 0 \\ 0 & c_{23} & s_{23} \\ 0 & -s_{23} & c_{23} \end{bmatrix} \begin{bmatrix} c_{13} & 0 & s_{13}e^{-i\delta} \\ 0 & 1 & 0 \\ -s_{13}e^{i\delta} & 0 & c_{13} \end{bmatrix} \begin{bmatrix} c_{12} & s_{12} & 0 \\ -s_{12} & c_{12} & 0 \\ 0 & 0 & 1 \end{bmatrix} \begin{bmatrix} e^{i\alpha_1/2} & 0 & 0 \\ 0 & e^{i\alpha_2/2} & 0 \\ 0 & 0 & 1 \end{bmatrix} \\
&= \begin{bmatrix} c_{12}c_{13} & s_{12}c_{13} & s_{13}e^{-i\delta} \\ -s_{12}c_{23} - c_{12}s_{23}s_{13}e^{i\delta} & c_{12}c_{23} - s_{12}s_{23}s_{13}e^{i\delta} & s_{23}c_{13} \\ s_{12}s_{23} - c_{12}c_{23}s_{13}e^{i\delta} & -c_{12}s_{23} - s_{12}c_{23}s_{13}e^{i\delta} & c_{23}c_{13} \end{bmatrix} \begin{bmatrix} e^{i\alpha_1/2} & 0 & 0 \\ 0 & e^{i\alpha_2/2} & 0 \\ 0 & 0 & 1 \end{bmatrix},
\end{aligned}
$$

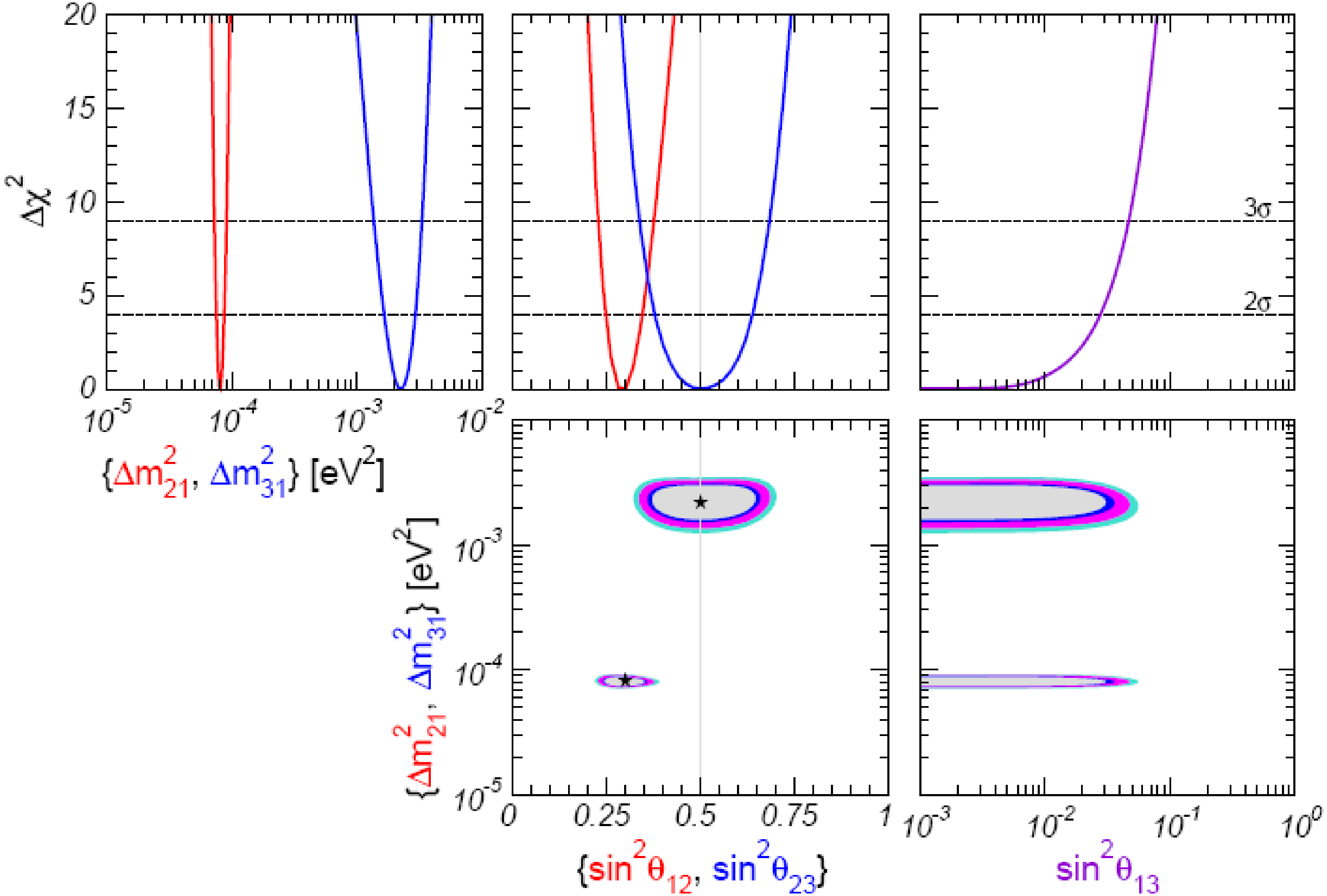

Δχ²
20
15
10
5
0
3σ
2σ
10⁻⁵
10⁻⁴
10⁻³
10⁻²
{Δm²₂₁, Δm²₃₁} [eV²]
{Δm²₂₁, Δm²₃₁} [eV²]
10⁻⁵
10⁻⁴
10⁻³
10⁻²
0
0.25
0.5
0.75
1
{sin²θ₁₂, sin²θ₂₃}
10⁻³
10⁻²
10⁻¹
10⁰
sin²θ₁₃

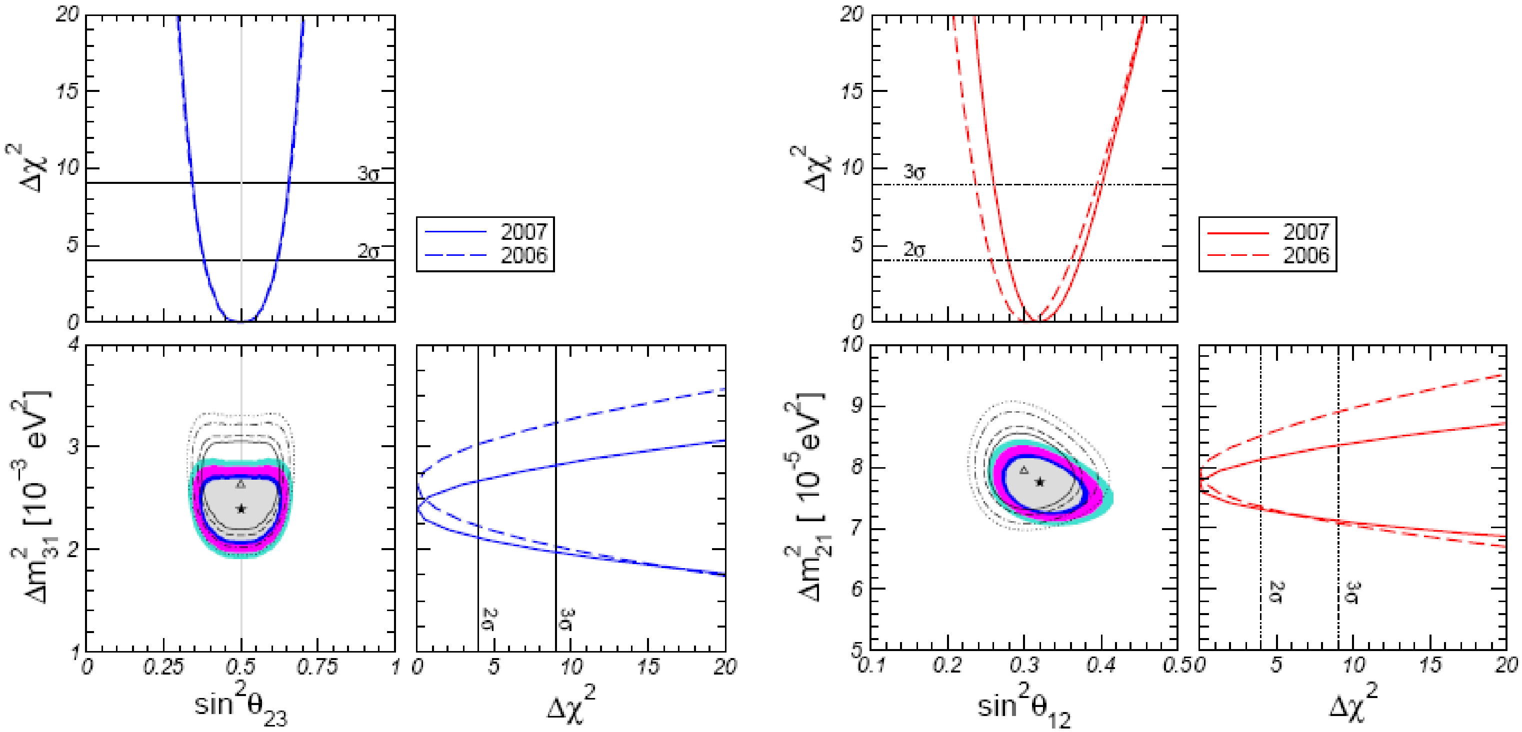

Figure D1. Left: Allowed region in the $(\sin^2\theta_{23}, \Delta m^2_{31})$ plane before (lines) and after (coloured regions) the inclusion of the new MINOS data. Right: Allowed region in the $(\sin^2\theta_{12}, \Delta m^2_{21})$ plane before (lines) and after (coloured regions) the inclusion of the new KamLAND data.

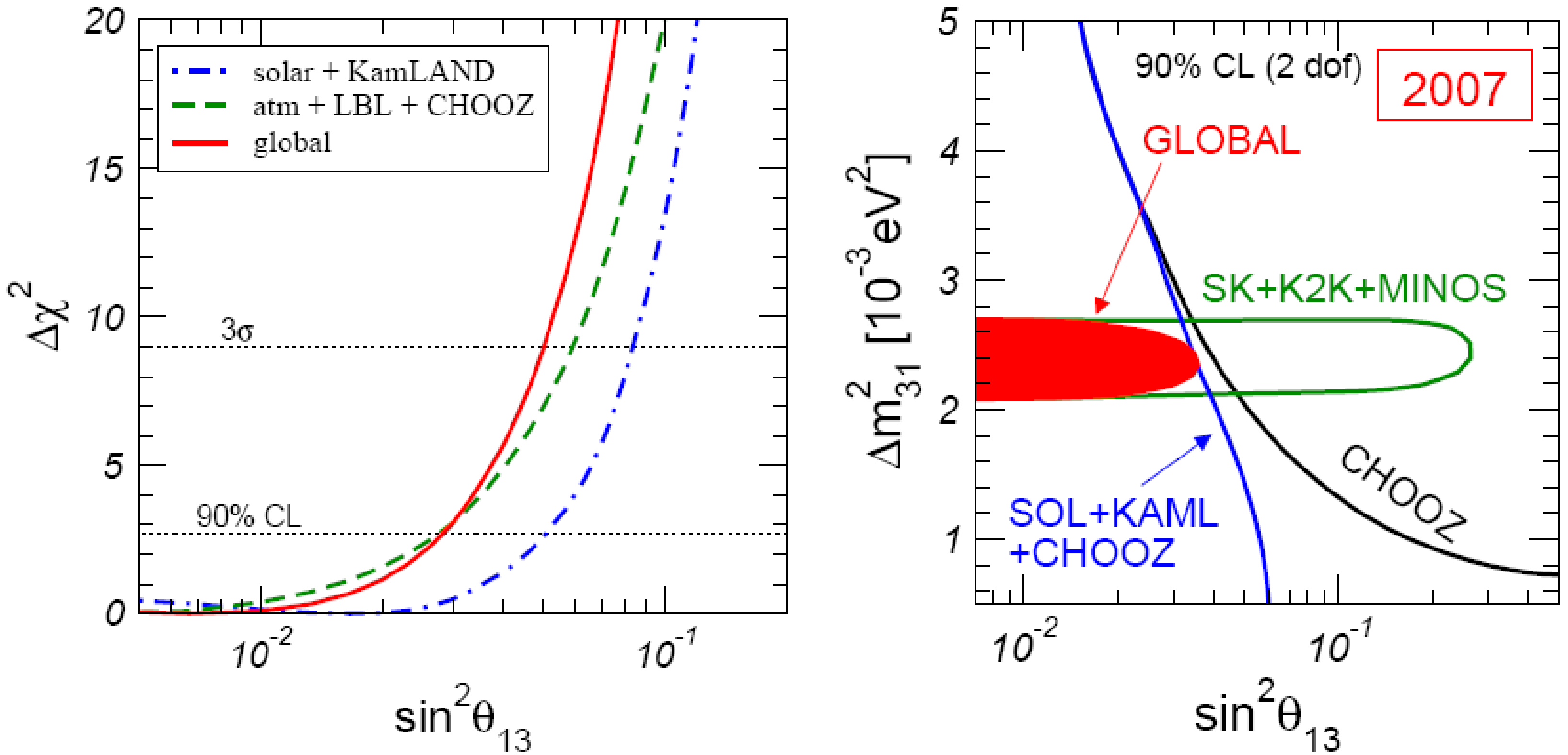
solar + KamLAND
atm + LBL + CHOOZ
global
3σ
90% CL
$\Delta\chi^2$
$\sin^2\theta_{13}$
90% CL (2 dof)
2007
GLOBAL
SK+K2K+MINOS
CHOOZ
SOL+KAML
+CHOOZ
Δm^2_{31} [10^{-3} eV^2]
$\sin^2\theta_{13}$

parameter	best fit	2σ	3σ
Δm^2_{21} $[10^{-5}\text{eV}^2]$	7.6	7.3–8.1	7.1–8.3
Δm^2_{31} $[10^{-3}\text{eV}^2]$	2.4	2.1–2.7	2.0–2.8
$\sin^2\theta_{12}$	0.32	0.28–0.37	0.26–0.40
$\sin^2\theta_{23}$	0.50	0.38–0.63	0.34–0.67
$\sin^2\theta_{13}$	0.007	≤ 0.033	≤ 0.050

Table D1. `2007 updated version of Table 1`. Best-fit values, 2σ and 3σ intervals (1 d.o.f.) for the three–flavour neutrino oscillation parameters from global data including solar, atmospheric, reactor (KamLAND and CHOOZ) and accelerator (K2K and MINOS) experiments.

arxiv.org: hep-ph/0405172 v6

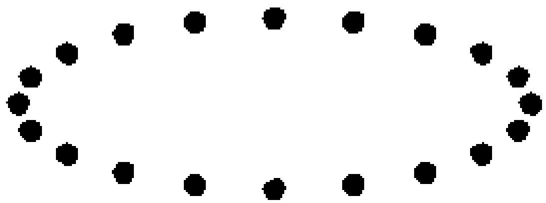
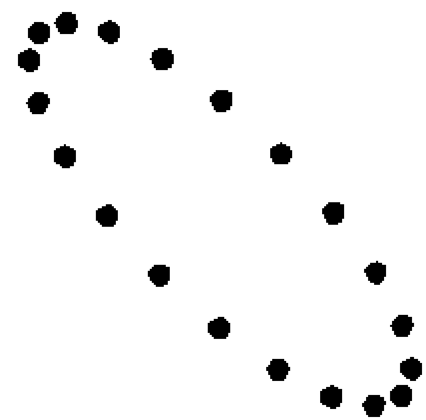

Spin-Powered Pulsars: A Census

- Number of known pulsars: 1765
- Number of millisecond pulsars: 170
- Number of binary pulsars: 131
- Number of AXPs: 12
- Number of pulsars in globular clusters: 99*
- Number of extragalactic pulsars: 20

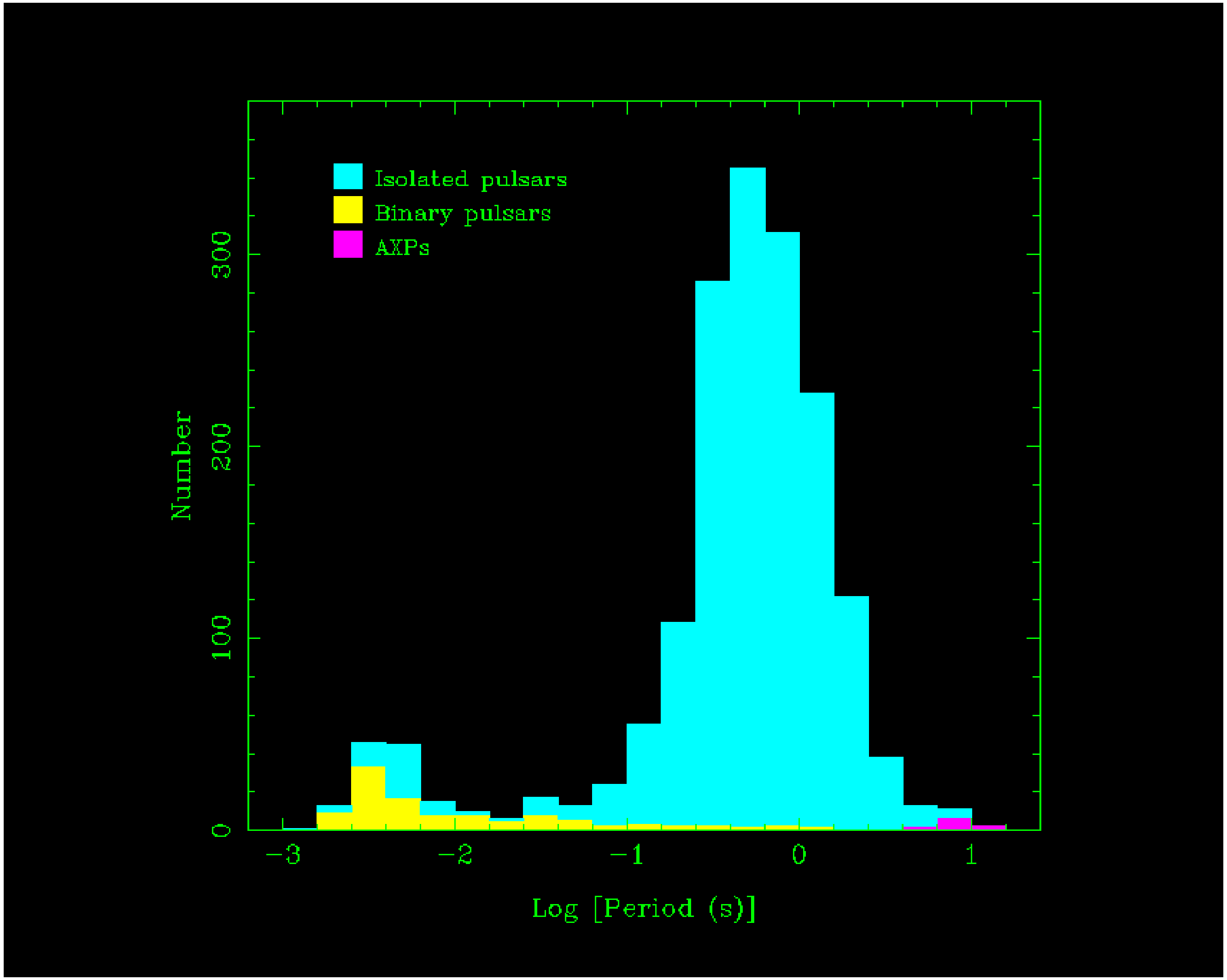

* Total known: 129 in 24 clusters
(Paulo Freire's web page)

Data from ATNF Pulsar Catalogue, V1.25
(www.atnf.csiro.au/research/pulsar/psrcat; Manchester et al. 2005)

P - Ṗ Diagram

- Millisecond pulsars have very low Ṗ and are very old
- Most MSPs are binary
- MSPs are formed by ‘recycling’ an old pulsar in an evolving binary system
- ‘Normal’ pulsars have significant period irregularities, but MSP periods are very stable

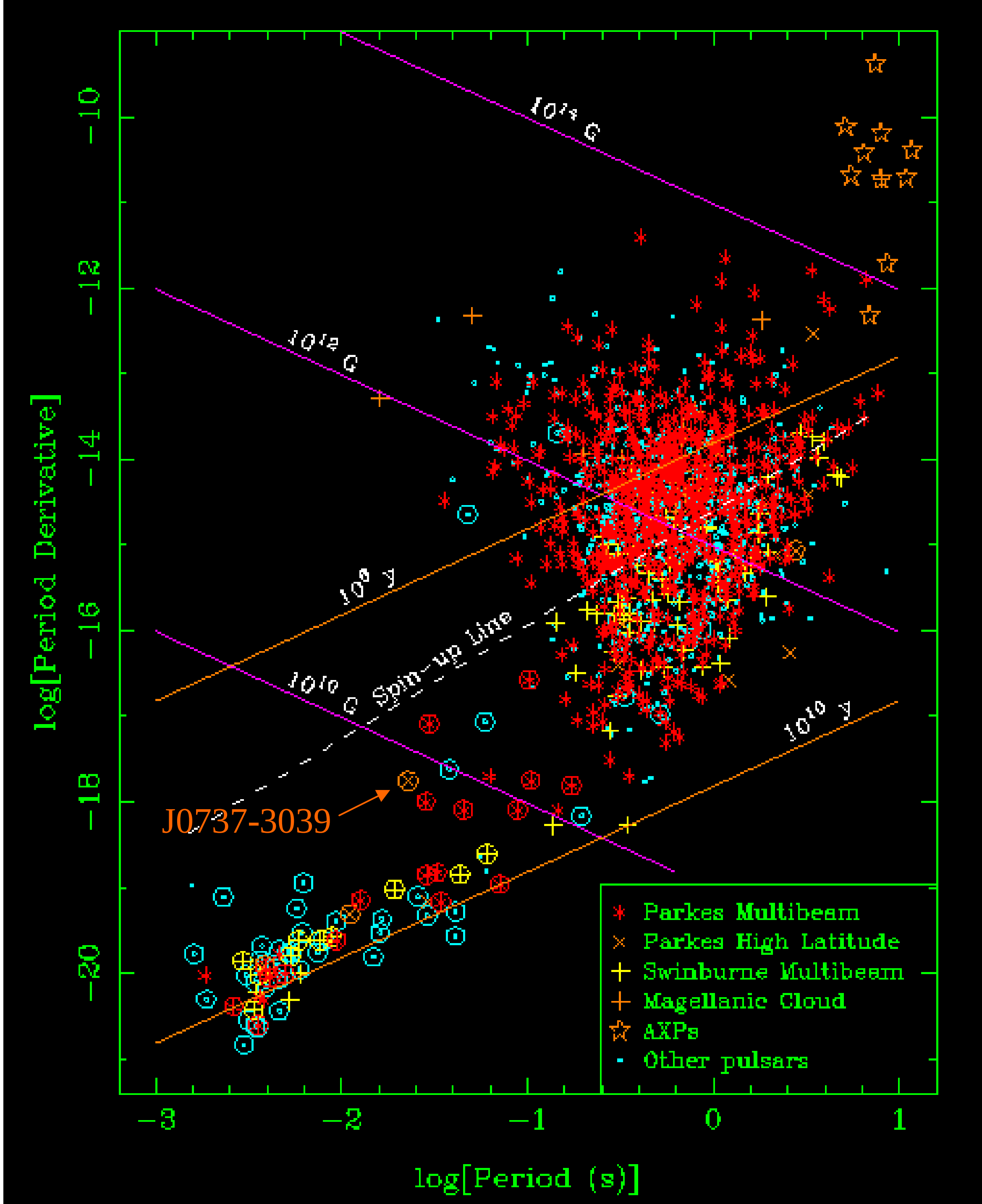

Pulsars and Gravitational Waves

Orbital decay in high-mass short-period binary systems accounted for by loss of energy to gravitational waves.

First observational evidence for gravitational waves!

Observed rates agree with the predictions of general relativity!

- PSR B1913+16: $\dot{P}_{b,obs}/\dot{P}_{b,pred}$ = 1.0013   0.0021

Precision of GR test limited by uncertainty in correction for acceleration in gravitational field of the Galaxy

(Weisberg & Taylor 2005)

- PSR B1534+12: $\dot{P}_{b,obs}/\dot{P}_{b,pred}$ = 0.91   0.05

Limited by uncertainty in pulsar distance;assuming GR gives improved distance estimate (Stairs et al. 2002)

- PSR J1141-6545: $\dot{P}_{b,obs}/\dot{P}_{b,pred}$ = 1.05   0.25

(NS-WD system) (Bailes et al. 2003)

- PSR J0737-3039A/B: $\dot{P}_{b,obs}/\dot{P}_{b,pred}$ = 1.004   0.014

Expect 0.1% test in ~5 years! (Kramer et al. 2006)

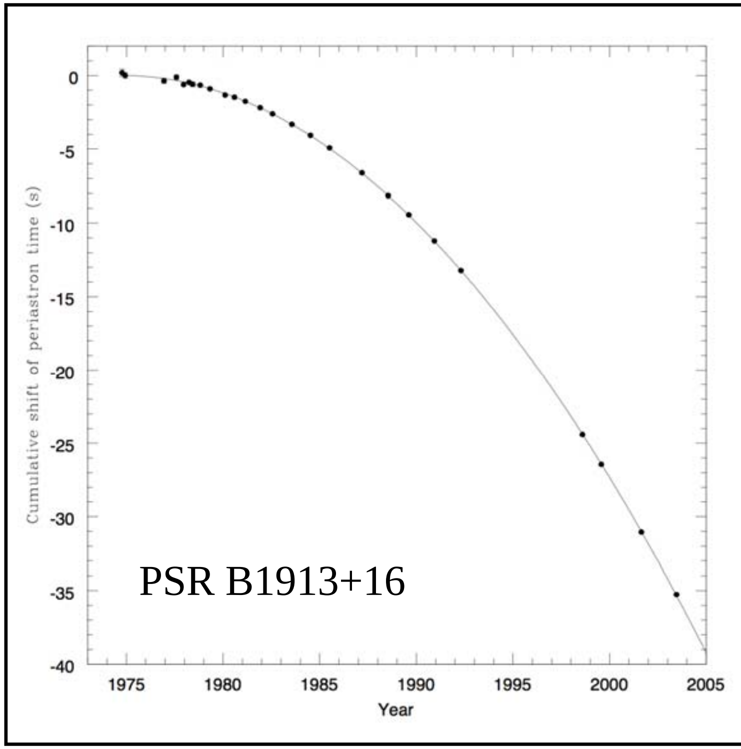

PSR J0737-3039A/B - the Double Pulsar

- Four times as relativistic as Hulse-Taylor binary pulsar
- Detection of both pulsars gives the mass ratio of the two stars
- Have measured five relativistic parameters in just two years!
- Four independent tests of general relativity
- Consistent at the 0.05% level!

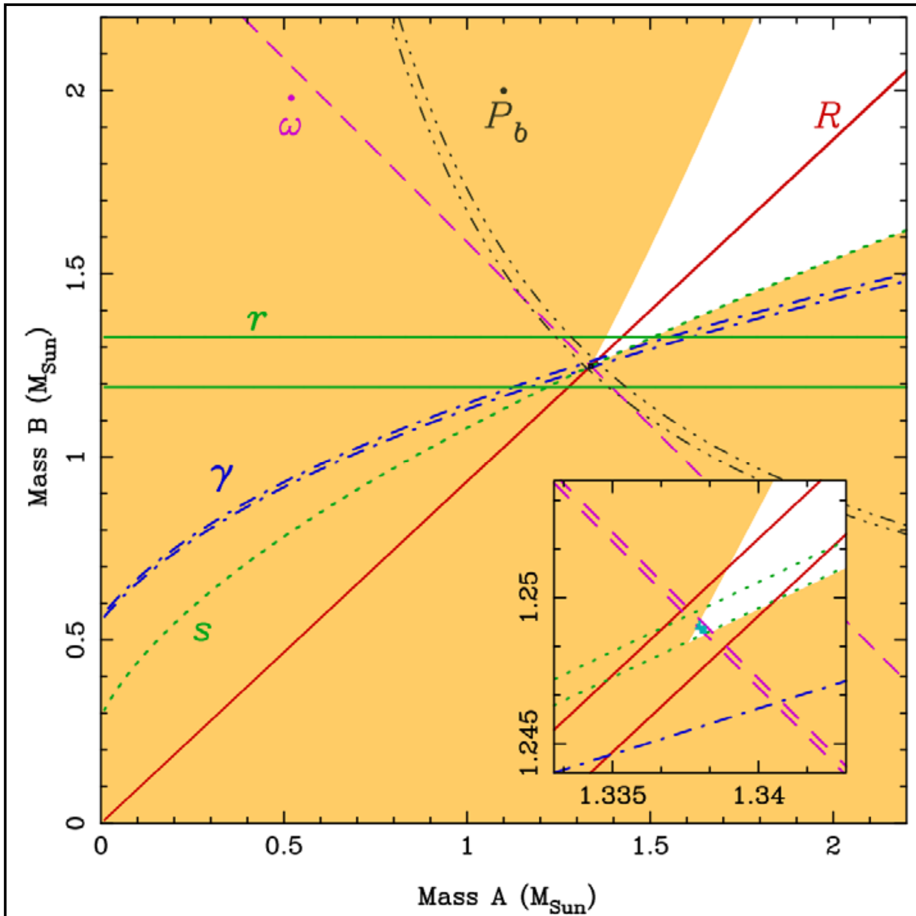

R: Mass ratio

: periastron advance

: gravitational redshift

r & s: Shapiro delay

P_b: orbit decay

(Kramer et al. 2006)

zdroj	amplitude	frekvence	typ signálu
supernova v Galaxii	10^{-18}	1 kHz	pulzní
supernova v LMC	10^{-19}	1 kHz	pulzní
supernova v Panně	10^{-21}	1 kHz	pulzní
srážka černých děr	10^{-20}	100 Hz	kvaziperiodický
srážka neutronových hvězd	10^{-22}	< 1 kHz	kvaziperiodický
vibrace černé díry	?	< 10 kHz	tlumené oscilace
velký třesk	?	?	šum

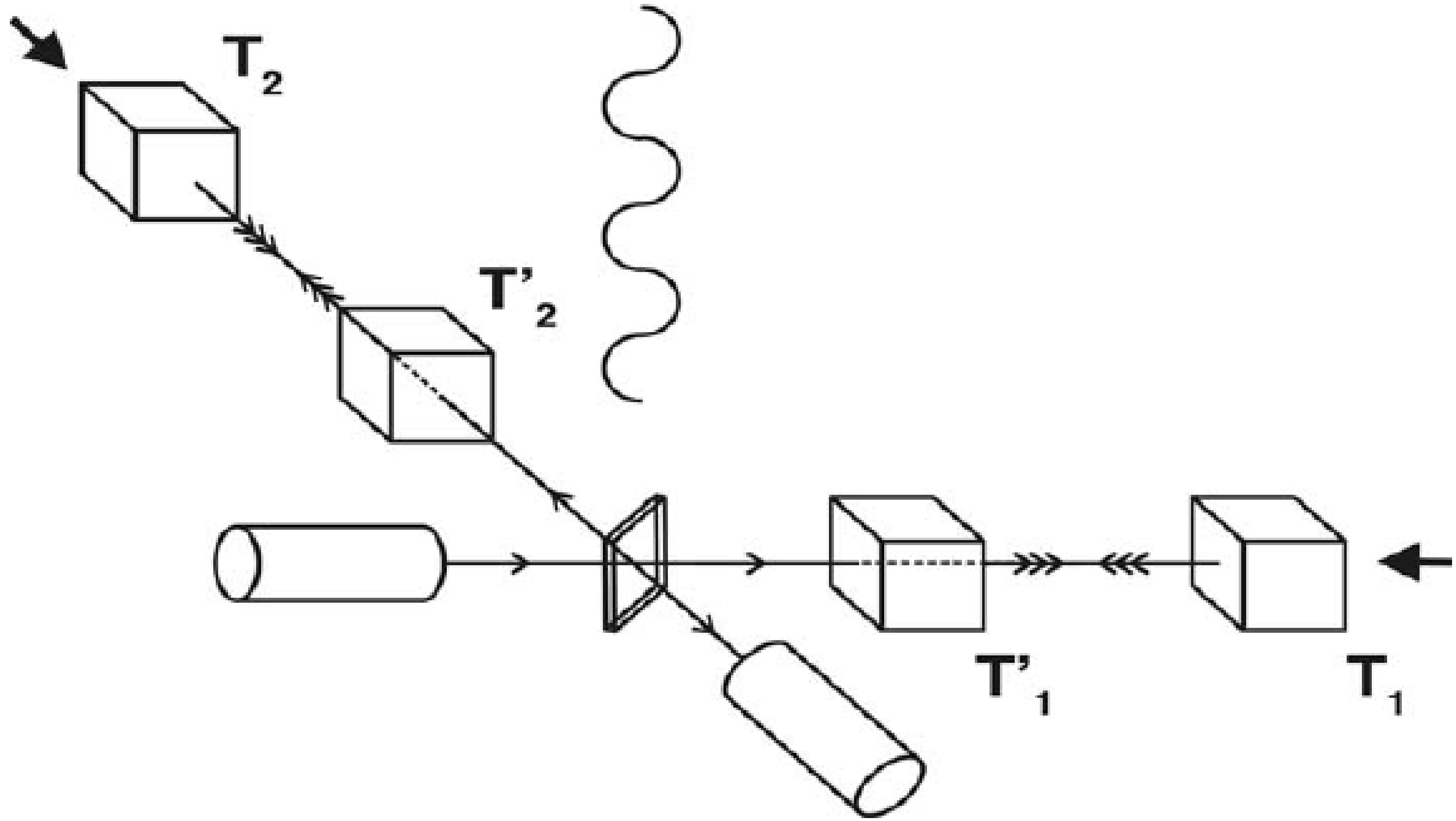

Obrázek 2 – Interferometry projektu LIGO budou dosahovat vyšší citlivosti zásluhou Fabryho-Perotových rezonančních dutin. Paprsky se budou v obou ramenech mnohonásobně odrážet mezi volně zavěšenými tělesy T_1 a T'_1 resp. T_2 a T'_2. Teprve poté se složí a dopadnou na fotodetektor.

název	umístění	země	rok	rozměr	www
MARK 2	Pasadena	USA	1991	40 m	www.ligo.caltech.edu
TAMA 300	Tokio	Japonsko	2000	300 m	tamago.mtk.nao.ac.jp
GEO 600	Hannover	SRN, GB	2001	600 m	www.geo600.uni-hannover.de
LIGO	Hanford, Livingstone	USA	2002	4 km	www.ligo.caltech.edu
VIRGO	Pisa	Itálie, Francie	2003	3 km	www.virgo.infn.it
LISA	vesmír	ESA, NASA	2010?	5 mil km	sci.esa.int/lisa; lisa.jpl.nasa.gov

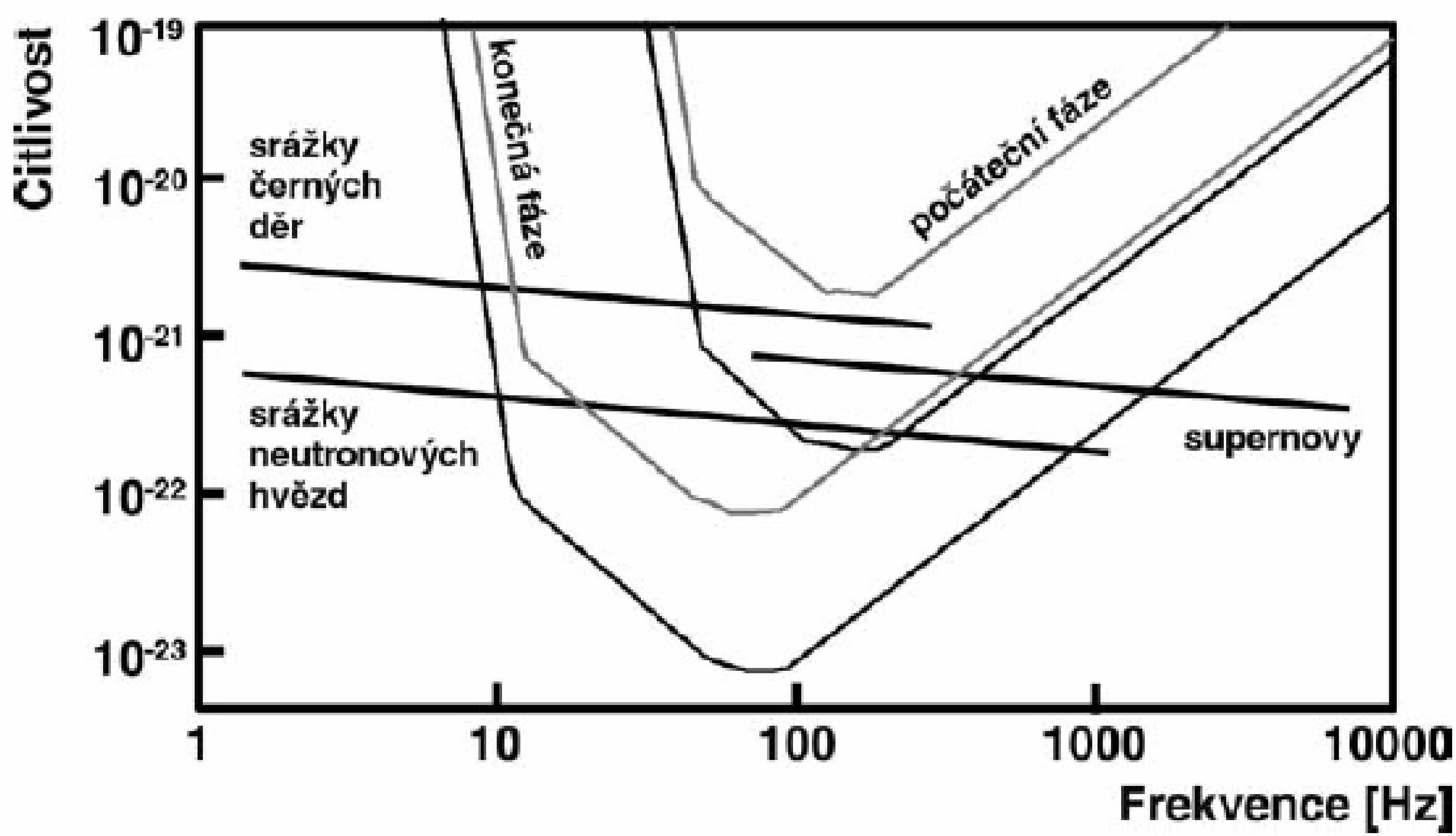
Citlivost
10^{-19}
10^{-20}
10^{-21}
10^{-22}
10^{-23}
srážky
černých
děr
srážky
neutronových
hvězd
konečná fáze
počáteční fáze
supernovy
1
10
100
1000
10000
Frekvence [Hz]

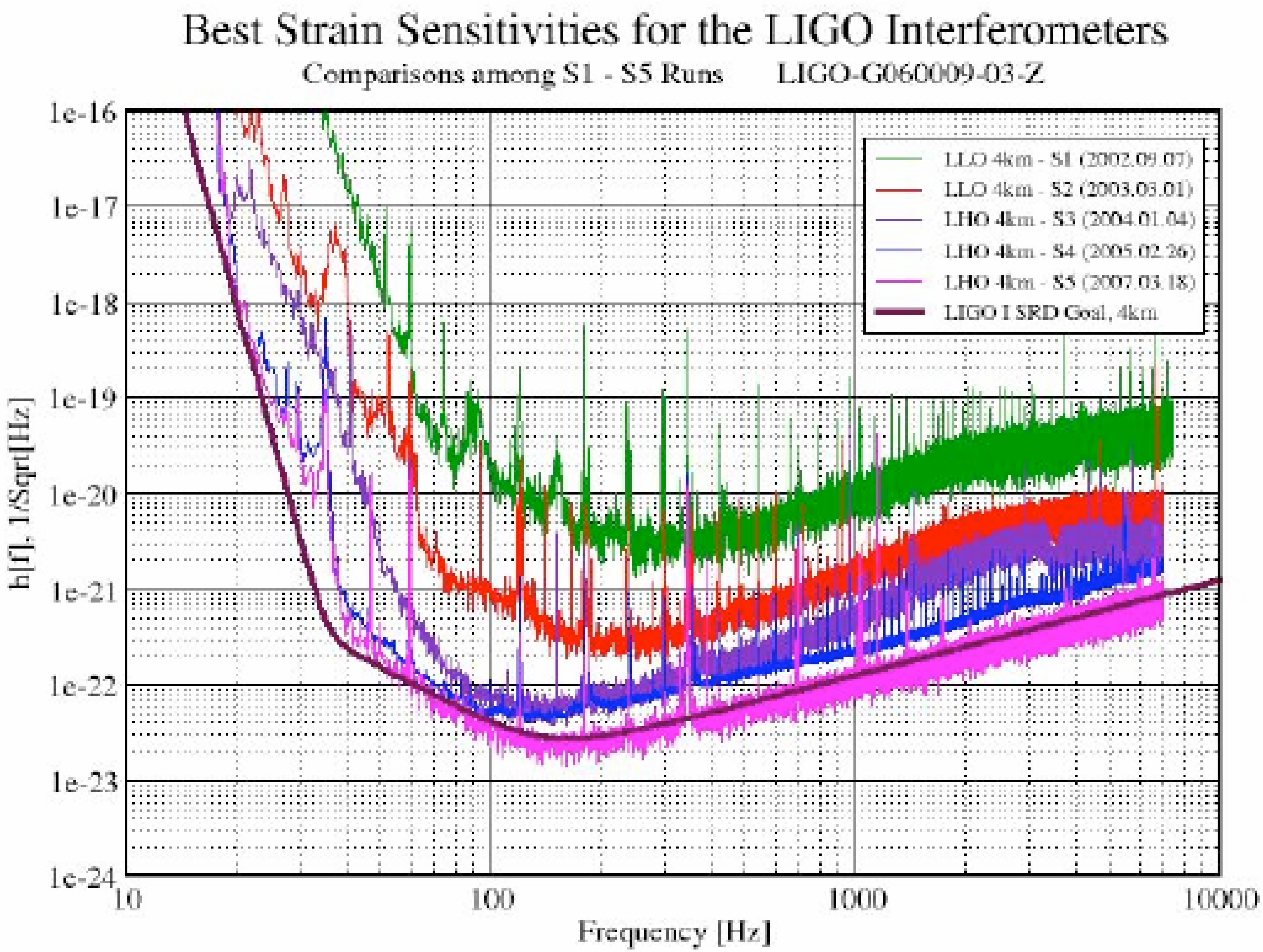

Best Strain Sensitivities for the LIGO Interferometers
Comparisons among S1 - S5 Runs LIGO-G060009-03-Z
LLO 4km - S1 (2002.09.07)
LLO 4km - S2 (2003.03.01)
LHO 4km - S3 (2004.01.04)
LHO 4km - S4 (2005.02.26)
LHO 4km - S5 (2007.03.18)
LIGO I SRD Goal, 4km
h[f], 1/Sqrt[Hz]
1e-16
1e-17
1e-18
1e-19
1e-20
1e-21
1e-22
1e-23
1e-24
10
100
1000
10000
Frequency [Hz]

LISA: Laser Interferometer Space Antenna

- ESA – NASA project
- Orbits Sun, 20° behind the Earth
- Three spacecraft in triangle, 5 million km each side
- Sensitive to GW signals in the range 10^{-4} – 10^{-1} Hz
- Planned launch ~2015

Most probable astrophysical sources: Compact stellar binary systems in our Galaxy and merger of binary black holes in cores of galaxies

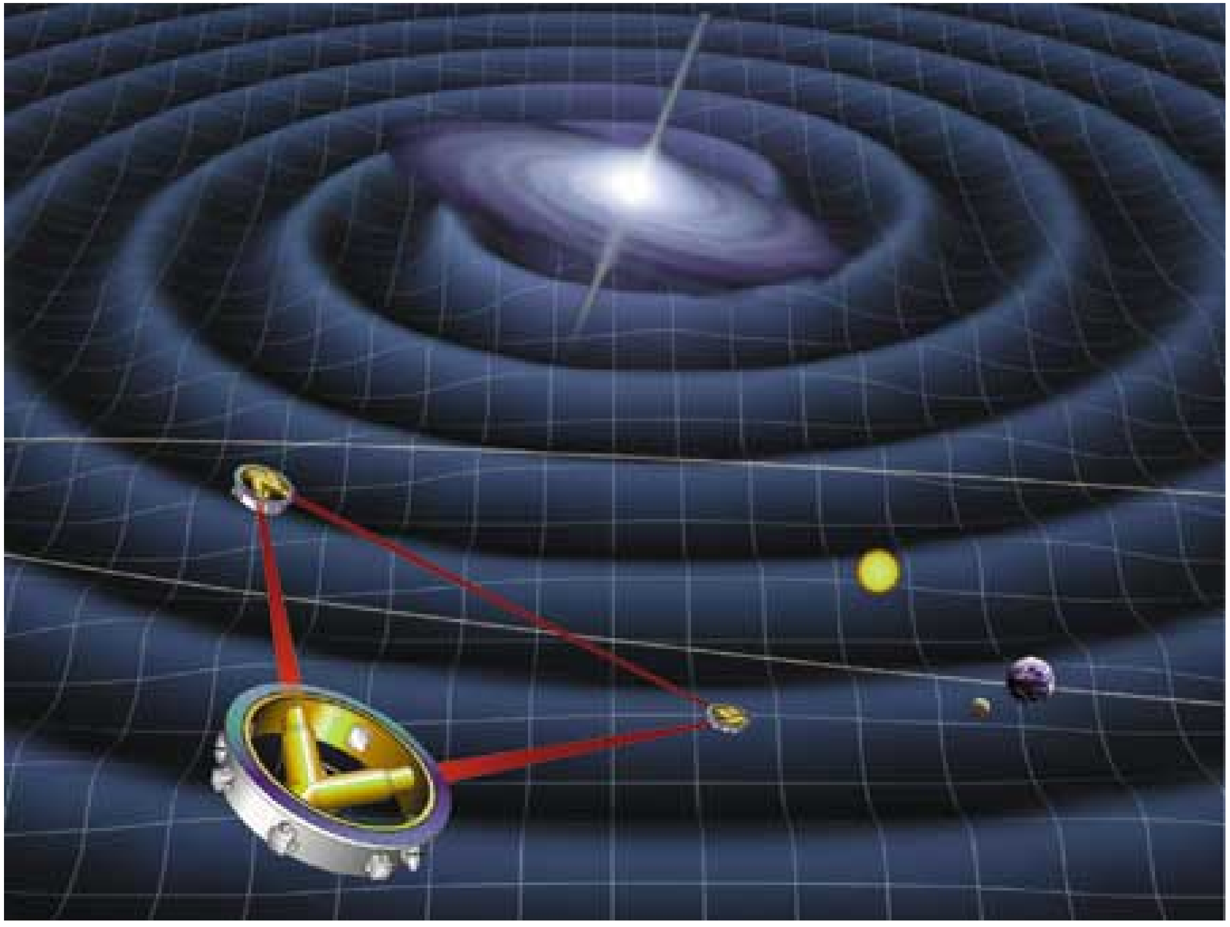

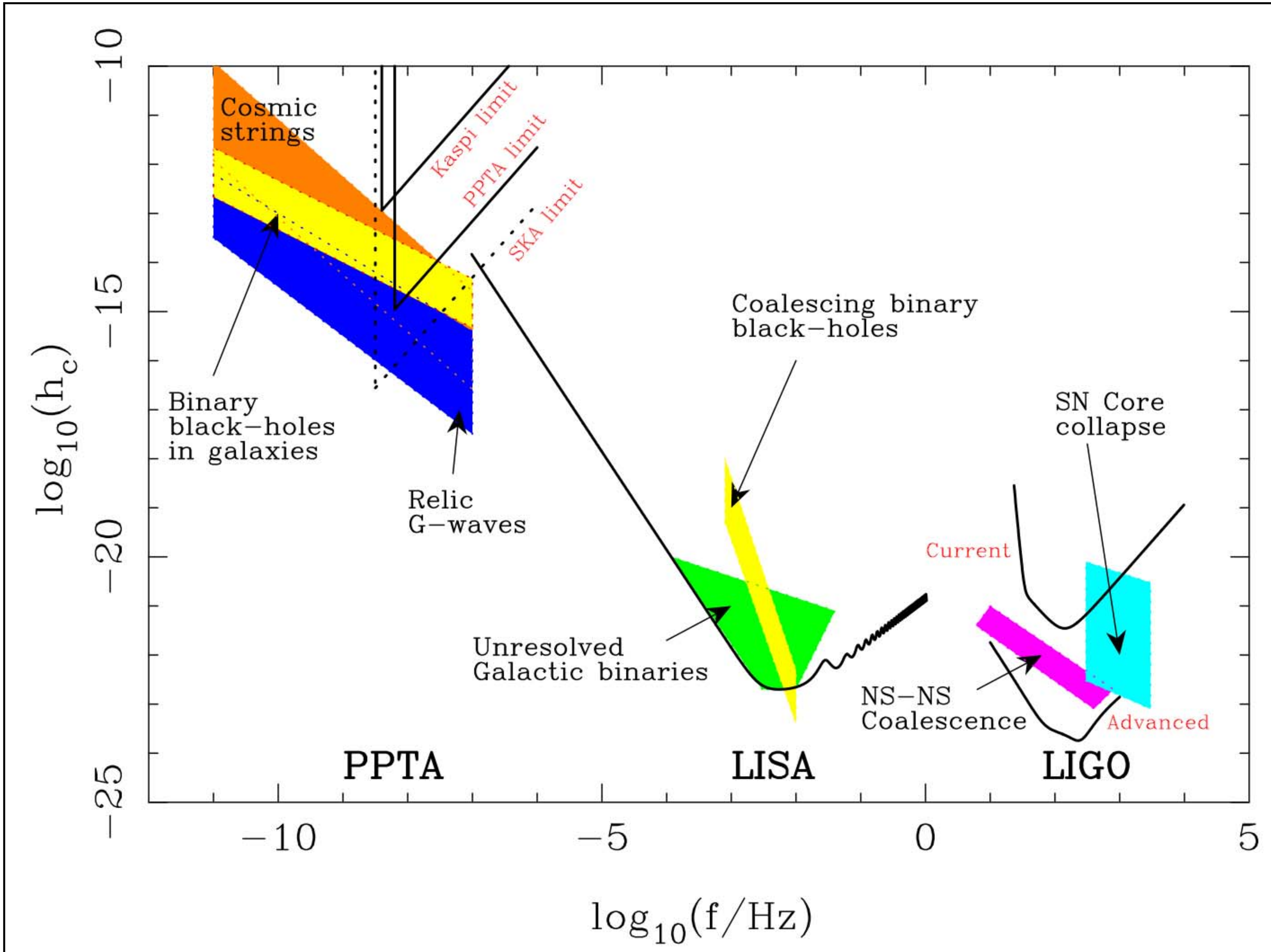

Cosmic strings
Kaspi limit
PPTA limit
SKA limit
Binary black−holes in galaxies
Relic G−waves
Coalescing binary black−holes
SN Core collapse
Current
Unresolved Galactic binaries
NS−NS Coalescence
Advanced
PPTA
LISA
LIGO
−10
−15
−20
−25
−5
0
5
$\log_{10}(h_c)$
$\log_{10}(f/Hz)$

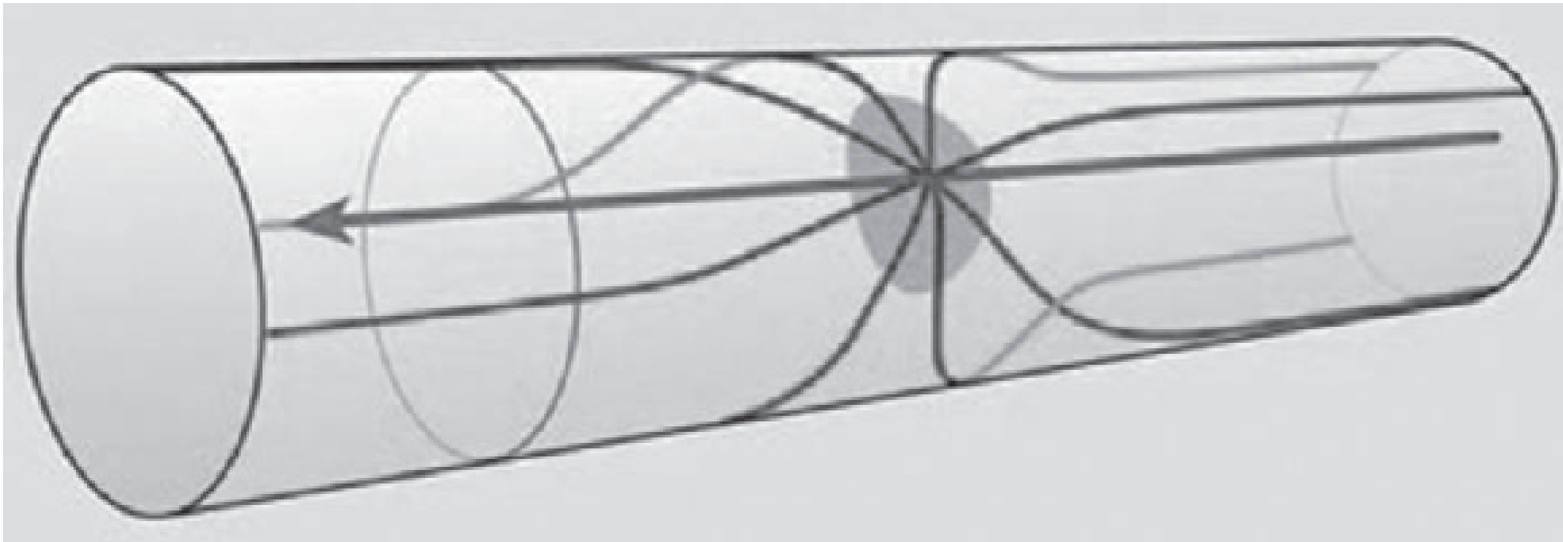

© E. Adelberger et al., physicsworld.com

Gaussův zákon a extradimenze. Gaussův zákon říká, že síla nekonečného dosahu (třeba gravitační nebo elektromagnetická) klesá tak rychle, jak rychle řídnou její siločáry. V normálním třírozměrném prostoru tedy řídnou tak, jak narůstá plocha, tedy se vzdáleností na druhou. Pokud však náš prostoročas obsahuje i nějakou „velkou“ extradimenzi – v obrázku je vyznačena průměrem válce – bude všechno jinak. Pokud budeme měřit na rozměru menším, než je rozměr extradimenze, bude intenzita gravitace klesat rychleji – siločáry budou mít rozměr navíc, ve kterém se mohou rozptylovat. Na větších vzdálenostech ale už budou siločáry v „extra“ rozměru rovnoběžné a budou klesat jen se čtvercem vzdálenosti, jak je obvyklé. Obecné pravidlo je jednoduché, v prostoru s n dimenzemi síla klesá s (n-1). mocninou vzdálenosti. Budou-li tedy extradimenze dvě, pak čekejme na menším než charakteristickém rozměru klesání intenzity se čtvrtou mocninou vzdálenosti.

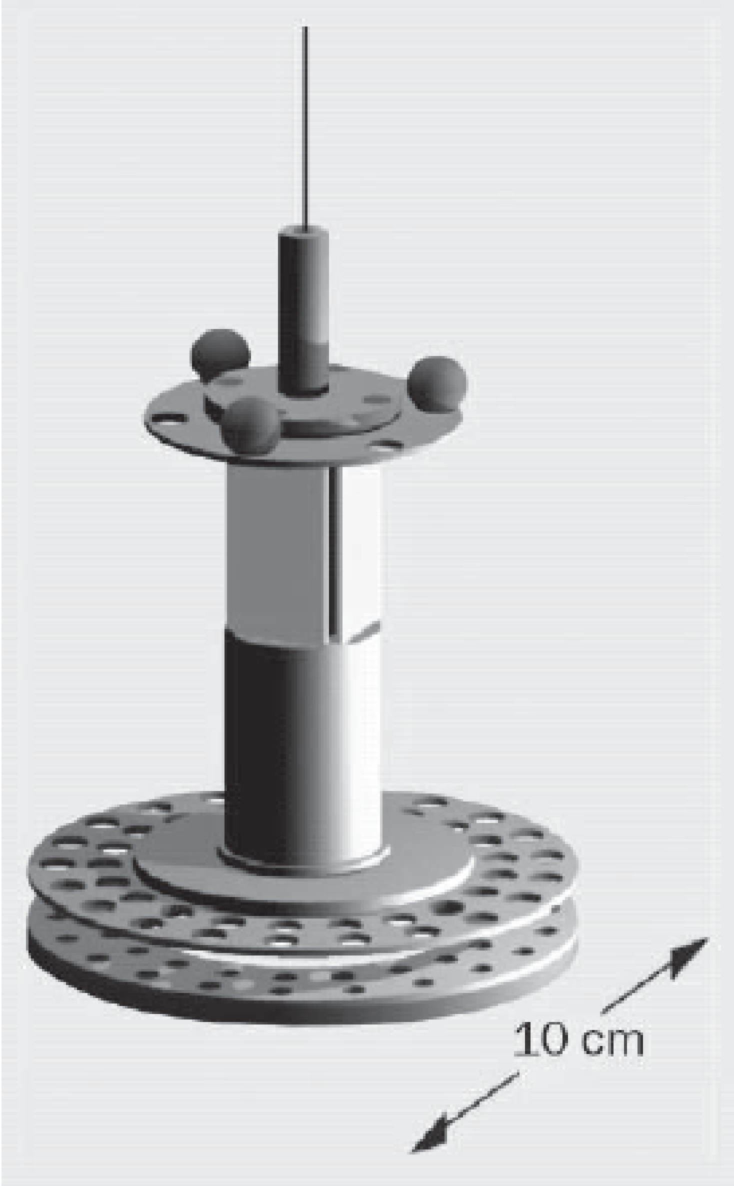
10 cm

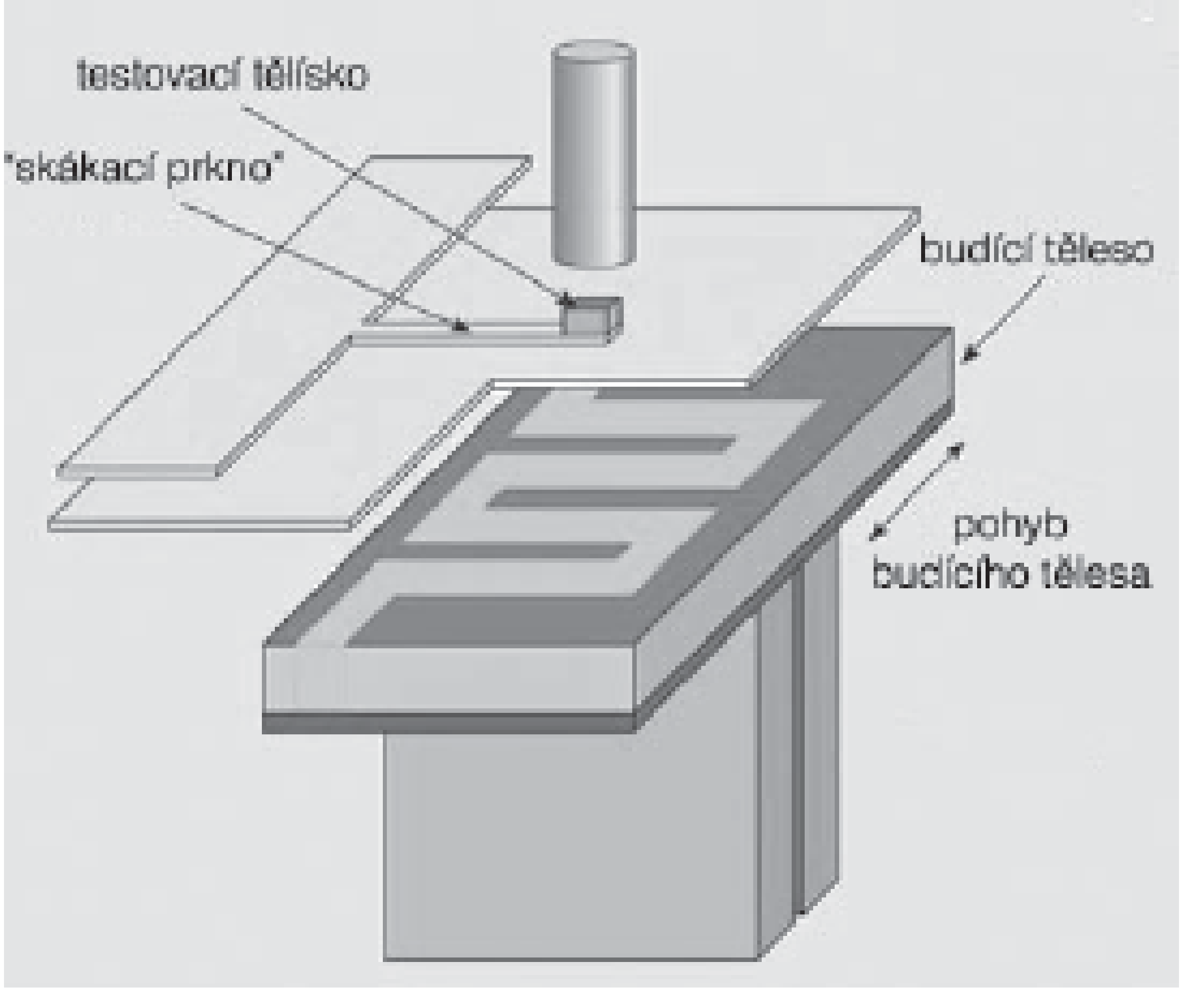
testovací tělísko
"skákací prkno"
budící těleso
pohyb
budícího tělesa

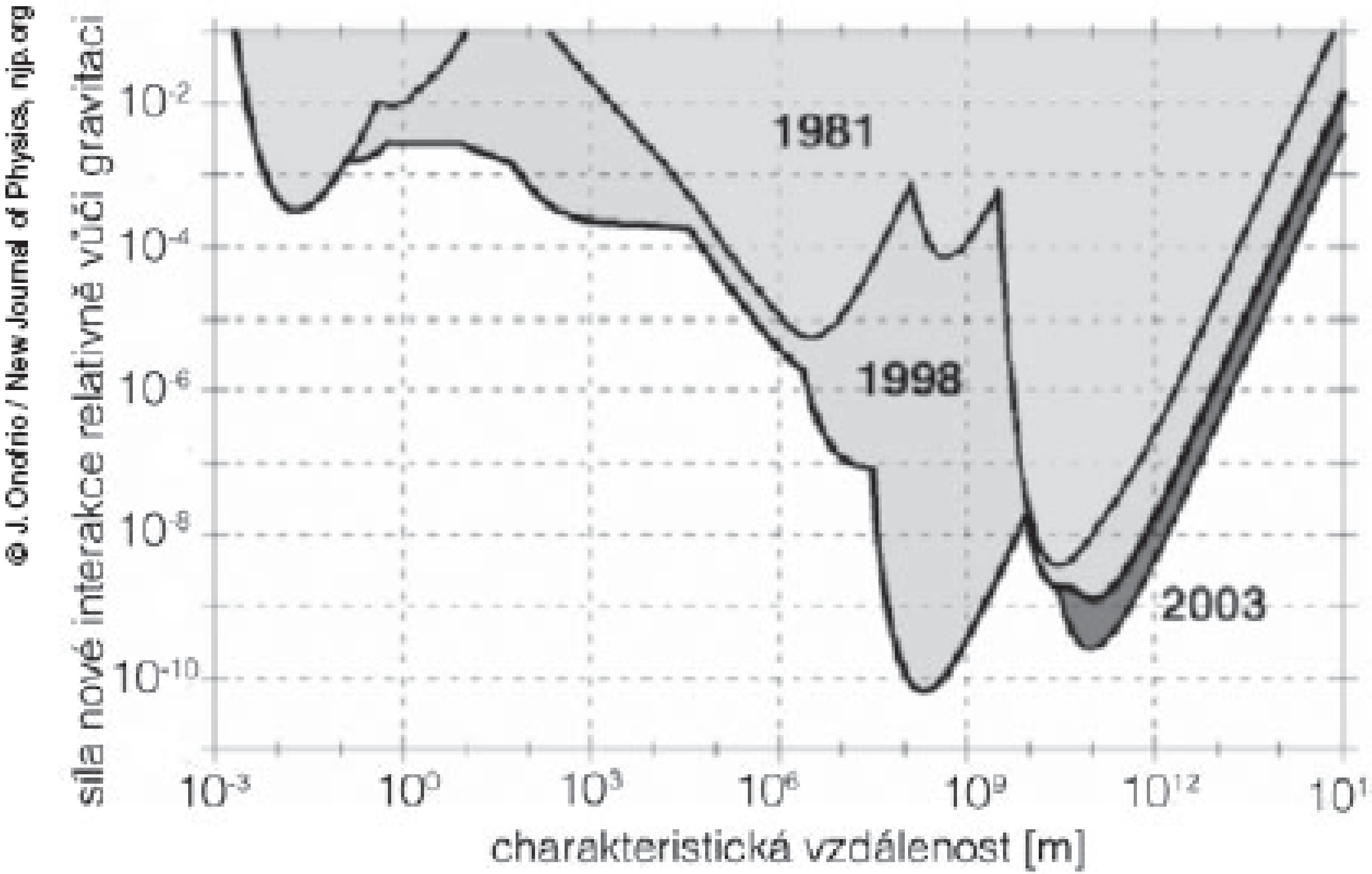
© J. Ondrio / New Journal of Physics, njp.org
síla nové interakce relativně vůči gravitaci
charakteristická vzdálenost [m]
1981
1998
2003
10^{-2}
10^{-4}
10^{-6}
10^{-8}
10^{-10}
10^{-3}
10^{0}
10^{3}
10^{6}
10^{9}
10^{12}
10^{15}

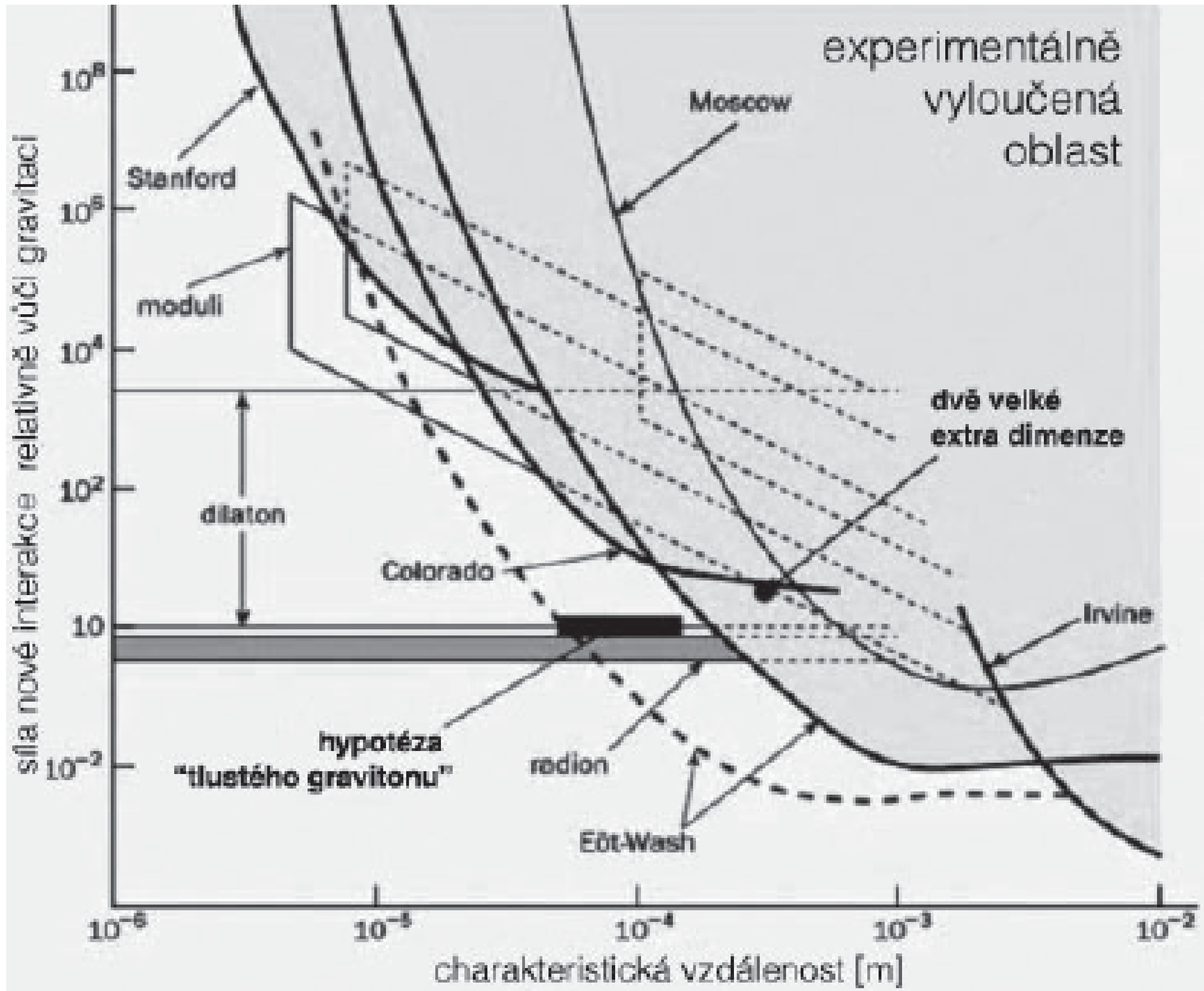
experimentálně
vyloučená
oblast
Moscow
Stanford
moduli
dilaton
Colorado
dvě velké
extra dimenze
Irvine
hypotéza
"tlustého gravitonu"
radion
Eöt-Wash
síla nové interakce relativně vůči gravitaci
10^{8}
10^{6}
10^{4}
10^{2}
10
10^{-2}
10^{-6}
10^{-5}
10^{-4}
10^{-3}
10^{-2}
charakteristická vzdálenost [m]

Varying Constants

John D. Barrow
DAMTP
Centre for Mathematical Sciences
Cambridge University
Cambridge CB3 0WA
UK

February 5, 2008

Abstract

We review properties of theories for the variation of the gravitation and fine structure 'constants'. We highlight some general features of the cosmological models that exist in these theories with reference to recent quasar data that are consistent with time-variation in the fine structure 'constant' since a redshift of 3.5. The behaviour of a simple class of varying-alpha cosmologies is outlined in the light of all the observational constraints.

1 Introduction

There are several reasons why the possibility of varying constants should be taken seriously [1]. First, we know that the best candidates for unification of the forces of nature in a quantum gravitational environment only seem to exist in finite form if there are many more dimensions of space than the three that we are familiar with. This means that the true constants of nature are defined in higher dimensions and the three-dimensional shadows we observe are no longer fundamental and do not need to be constant. Any slow change in the scale of the extra dimensions would be revealed by measurable changes in our three-dimensional 'constants'. Second, we appreciate that some apparent constant might be determined partially or completely by spontaneous symmetry-breaking processes in the very early universe. This introduces an irreducibly random element into the values of those constants. They may be different in different parts of the universe. The most dramatic manifestation of this process is provided by the chaotic and eternal inflationary universe scenarios where both the number and the strength of forces in the universe at low energy can fall out differently in